Chemosphere 310 (2023) 136805

Contents lists available at ScienceDirect

Chemosphere

journal homepage: www.elsevier.com/locate/chemosphere

The aggregation of natural inorganic colloids in aqueous environment: A review

Yihui Guo [a,b,1], Ning Tang [a,b,1], Jiayin Guo [a,b], Lan Lu [a,b], Na Li [a,b], Tingting Hu [a,b], Ziqian Zhu [a,b], Xiang Gao [a,b], Xiaodong Li [a,b], Longbo Jiang [a,b], Jie Liang [a,b,*]

[a] College of Environmental Science and Engineering, Hunan University, Changsha, 410082, PR China
[b] Key Laboratory of Environment Biology and Pollution Control, Hunan University, Ministry of Education, Changsha, 410082, PR China

HIGHLIGHTS

- The aggregation behaviors of NICs in water environment are systematically reviewed.
- Typical NICs are introduced in terms of structure, morphology, charge proprieties.
- The classical and extended DLVO interaction mechanisms are summarized elaborately.
- Both the intrinsic and extrinsic factors affecting NICs fate are analyzed in detail.
- The existing drawbacks and the future research directions are reasonably put forward.

GRAPHICAL ABSTRACT

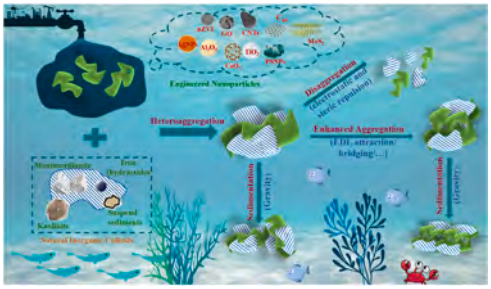

ARTICLE INFO

Handling Editor: Milena Horvat

Keywords:
Natural inorganic colloids
Aggregation behavior
X-DLVO theory
Natural organic matters
Aqueous environment

ABSTRACT

Natural inorganic colloids (NICs) are the most common and dominant existence in the ecosystem, with high concentration and wide variety. In spite of the low toxicity, they can alter activity and mobility of hazardous engineered nanoparticles (ENPs) through different interactions, which warrants the necessity to understand and predict the fate and transport of NICs in aquatic ecosystems. Here, this review summarized NICs properties and behaviors, interaction mechanisms and environmental factors at the first time. Various representative NICs and their physicochemical properties were introduced across the board. Then, the aggregation and sedimentation behaviors were discussed systematically, mainly concerning the heteroaggregation between NICs and ENPs. To speculate their fate and elucidate the corresponding mechanisms, the classical Derjaguin-Landau-Verwey-Overbeek (DLVO) and extended DLVO (X-DLVO) theories were focused. Furthermore, a range of intrinsic and extrinsic factors was presented in different perspective. Last but not the least, this paper pointed out theoretical and analytical gaps in current researches, and put forward suggestions for further research, aiming to provide a more comprehensive and original perspective in the fields of natural occurring colloids.

* Corresponding author. College of Environmental Science and Engineering, Hunan University, Changsha, 410082, PR China.
E-mail addresses: gyh2009@hnu.edu.cn (Y. Guo), liangjie@hnu.edu.cn (J. Liang).
[1] These authors contribute equally to this article.

https://doi.org/10.1016/j.chemosphere.2022.136805
Received 31 July 2022; Received in revised form 27 September 2022; Accepted 5 October 2022
Available online 9 October 2022

1. Introduction

Natural colloids (NCs, 1–1000 nm in diameter) were produced by natural substances through weathering and mineral formation processes, having been existed since 4.54 billion years ago (Sharma et al., 2015). While engineered nanoparticles (ENPs, 1–100 nm) just appeared after human activities (Hochella et al., 2019). Most of the present work has researched into the toxicity, transformation and behavior of ENPs, as their massive emissions can arise serious environmental concerns (Philippe and Schaumann, 2014; Peijnenburg et al., 2015). However, the behaviors of NCs were nonetheless neglected, which should be worth explorations and discussions. For the reasons that in generally, the annual production of NCs was approximately five to six magnitudes more than ENPs (Hochella et al., 2015; Sharma et al., 2015). Besides, it interacted with poisonous ENPs in a high probability to reduce the uncertainty of migration and occurrence for ENPs (Bakshi et al., 2015), further shrinking the risks of poison entering into creatures and environment to guarantee food safety and human health (Fig. 1).

The natural inorganic colloids (NICs), the major part of NCs, mainly included (1) clay minerals (e.g., montmorillonite (Zhou et al., 2012; Sabaraya et al., 2021) and kaolinite (Tombácz and Szekeres, 2006; Wang et al., 2015b)); (2) iron (hydr)oxides (e.g., hematite (He et al., 2008; Huynh et al., 2012), magnetite (Vikesland et al., 2016; Zhang et al., 2020), goethite (Vindedahl et al., 2016; Carstens et al., 2021) and Ferrihydrite); (3) suspend sediments (SS) and so forth (Zhao et al., 2021a), which were generally chosen as representative NICs to conduct researches and reviews due to their wide distributions. Their environmental behaviors, such as aggregation, disaggregation and sedimentation, are closely related to the stability in waters (Phenrat et al., 2007). Aggregation is the process that particles collide, attach and then produce larger clusters, while disaggregation and sedimentation is that the production breaks up and settles down, respectively (Therezien et al., 2014). Concerning the subdivisions of aggregation, homoaggregation occurs between two particles similar in physicochemical characteristics, and heteroaggregation exists between different particles (Islam et al., 1995; Bansal et al., 2017). Further, to explicate the internal mechanism and speculate the fate of nanoparticles (NPs), DLVO theory was developed to calculate the net interaction energy in terms of balancing van der Waals (VDW) and electrical double-layer (EDL) forces (Boström et al., 2001; Xu et al., 2015b). X-DLVO theory was supplemented to fully express the interactions in the complex natural environment (Hotze et al., 2010; Keller et al., 2010).

These colloidal behaviors are strongly affected by the intrinsic (eg., particle size, morphology, structure, potential) and environmental factors (eg., pH, ionic strength (IS), natural organic matters (NOM) and microorganisms) (van Riemsdijk et al., 2006; Ma et al., 2020; Sun et al., 2021a). For example, the bare and surface modified NICs have respective performance ascribing to varying shapes and sizes (Ghosh et al., 2016). Solution pH affects particle behavior by changing surface potential. For most colloids, the potential might be reversed with pH increasing. And when the potential is zero, the corresponding pH is called pH_{PZC} or PZC (Table 1). Besides, at high ionic strength or valency, particles aggregate quickly owing to the adequate DEL compression, bridging or other favorable forces (Clavier et al., 2016; Cheng et al., 2020a). NOM has similar impacts on particle stability through bridging (Sheng et al., 2016b; Liu et al., 2020; Sun et al., 2020a). It also attaches onto particles to induce steric hindrance, making aggregation reversible and the structure dynamic (Philippe and Schaumann, 2014). The impacts of these environmental factors are complex. Thus, having a deep understanding on these factors helps to control particle behaviors (Wang et al., 2018a).

Few studies paid attention to the fate and transport of NICs (Peijnenburg et al., 2015; Mukherjee et al., 2016; Abbas et al., 2020), thus this paper was reviewed from the following aspects to provide a more comprehensive knowledge: 1) the physical and chemical properties of representative clay minerals and iron oxides; 2) the association of NICs themselves and with ENPs; 3) the behavior mechanisms and modelling in NICs stability that can explain and extrapolate the fate and transport; 4) the intrinsic and extrinsic factors that affect colloidal behaviors; 5) the discussions on the deficiencies of current researches and prospects for future research.

2. Representative minerals

2.1. Clay minerals

Clay minerals, whose shape is similar to rounds or pillows with a slightly hexagon-like modular structure, are composed of hydrated aluminosilicate, possessing the potential to interact with pollutants and ENPs (Jing et al., 2021; Wang et al., 2021b).

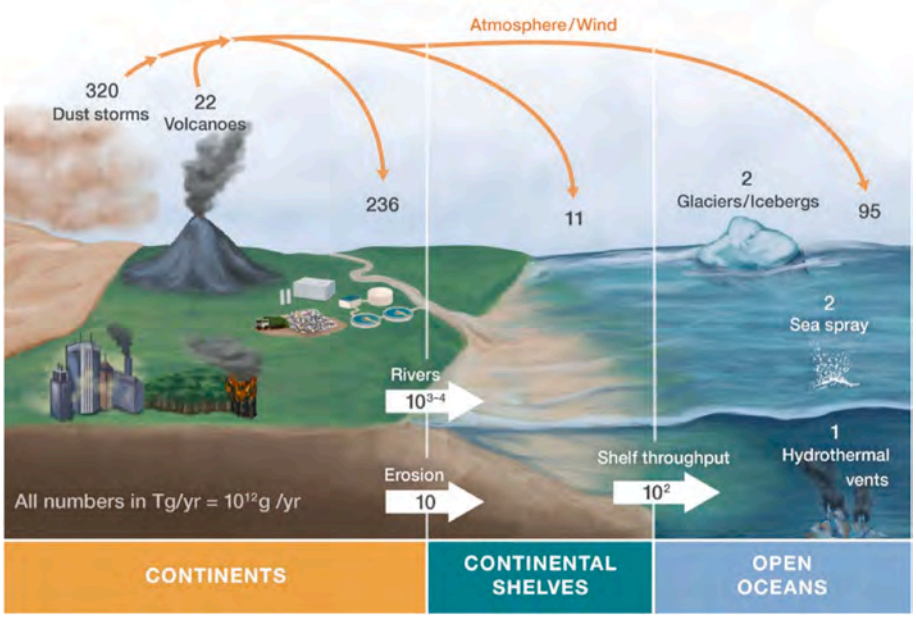

Fig. 1. Natural nanomaterials fluxes are described using black or white numbers, and within the bold white arrows for natural nanomaterials movement in the environment. Reproduced from (Hochella et al., 2019). Copyright (2019) Science.

Table 1
The pH_{PZC} s and CCCs of typical NICs under specific conditions.

Materials	pH_{PZC} (conditions)	Ref.	CCC (mM) (conditions)	Ref.
Kl	$pH_{PZC,\ edge}$ = 6 – 6.5 (100 mM NaCl)	Tombácz and Szekeres, (2006)	CCC_{NaCl} = 50, 150, 125 (pH = 4, 6, 8; size: 241 ± 114 nm)	Sabaraya et al., (2021)
	pH_{PZC} = 4.8 – 5.3 (10 mM NaCl)	Wang et al., (2019a)	CCC_{NaCl} = 263; CCC_{CaCl2} = 4	Wang et al., (2015b)
			CCC_{NaCl} = 50 (pH = 6.5)	Wang et al., (2019a)
Mt	$pH_{PZC,\ edge}$ ~ 6.5 (10 mM NaCl, size: 100 – 500 nm)	Zhou et al., (2012)	CCC_{NaNO3} = 35, 100 (pH = 4, 8; size: 100 – 500 nm)	Zhou et al., (2012)
	pH_{PZC} < 2.5 (10 mM NaCl)	Wang et al., (2019a)	CCC_{NaCl} = 37, 73, 147 (pH = 4, 6, 8; size: 357 ± 114 nm)	Sabaraya et al., (2021)
			CCC_{NaCl} = 80 (pH = 6.5)	Wang et al., (2019a)
Hematite	pH_{PZC} = 5.8 ± 0.1 (97.7 ± 2.5 nm)	Oriekhova and Stoll, (2019)	CCC_{NaCl} = 45 ± 4, 54 ± 6, 70 ± 6 (pH = 5.7; size: 12, 32, 65 nm)	He et al., (2008)
	pH_{PZC} = 7.2, 8.2, 8.8 (12, 32, 65 nm)	He et al., (2008)	CCC_{NaCl} = 35.7 (pH = 5.2; size: 87 nm)	Huynh et al., (2012)
	pH_{PZC} = 7.8–9.2	Philippe and Schaumann, (2014)	CCC_{NaCl} = 45.8 (pH = 5.2; size: 87–95 nm)	Feng et al., (2017)
	pH_{PZC} = 7.5 (140.8 nm)	Xu et al., (2015b)	CCC_{NaCl} = 75.0; CCC_{NaNO3} = 79.2; CCC_{NaF} = 7.8; CCC_{Na2SO4} = 0.5 (140.8 nm)	Xu et al., (2015b)
	pH_{PZC} = 7.8 (1 mM NaCl; size: 20 nm)	Baalousha, (2009)	CCC_{NaCl} = 69; CCC_{CaCl2} = 10 (pH = 5.7; size: 125 ± 18 nm)	Sheng et al., (2016b)
Goethite	pH_{PZC} = 8.0–9.0	Zhang et al., (2020)	CCC_{NaCl} = 62.6; CCC_{NaNO3} = 54.7; CCC_{NaF} = 5.5; CCC_{Na2SO4} = 0.2 (152.1 nm)	Xu et al., (2015b)
	pH_{PZC} = 7.0–8.0	Philippe and Schaumann, (2014)		
	pH_{PZC} = 7.9 (152.1 nm)	Xu et al., (2015b)		
H_{Asp} α-FeOOH	pH_{PZC} = 8.9	Ghosh et al., (2016)	CCC_{CaCl2} = 59 (pH = 5)	Ghosh et al., (2016)
L_{Asp} α-FeOOH	pH_{PZC} = 6.5	Ghosh et al., (2016)		
Magnetite	pH_{PZC} = 7.0–7.5; ~8	(Zhang et al., 2020) (Philippe and Schaumann, 2014)	CCC_{NaCl} = 23.8 (pH = 9.8; size: 12.2 ± 1.2 nm)	Hu et al., (2010b)
Ferridyrite	pH_{PZC} = ~8.2 ± 0.1 (18.7 ± 1.5 nm)	Liao et al., (2017)	CCC_{NaCl} = 233; CCC_{CaCl2} = 107; CCC_{Na2SO4} = 2 (pH = 5.0 ± 0.1)	Liu et al., (2019a)
	pH_{PZC} = 7.1 (5 mM $NaNO_3$, size: 30 nm)	Li et al., (2020b)	CCC_{NaCl} = 150 (pH = 5.5; size: 30 nm)	Li et al., (2020b)

The plate-like clay minerals have the unique charge heterogeneity, which originates from the layer structure that comprises tetrahedral silicate sheets and octahedral aluminum hydroxide sheets (Uddin, 2017; Awad et al., 2019). The SiO_4^{2-} unit of tetrahedral sheets are arranged by layers to a simple hexagonal network ($Si_2O_6(OH)_4$). While, the octahedral sheets ($Al_2(OH)_6$) center on the cations (eg., Al^{3+}) with six oxygens or hydroxyls besieging them (Fig. 2a). These layers are connected together sharing oxygen atoms (Zhou et al., 2012). Consisting of repeated layers, kaolinite (Kl) is a typical 1:1 lamellar silicate (Uddin, 2017), and montmorillonite (Mt) is a representative 2:1 clay with one layer of Al-octahedra sandwiched with two layers of Si-tetrahedra (Fig. 2b) (Tombácz and Szekeres, 2006). The basal plane of Mt exhibits permanent net negative charges, owing to the isomorphic substitutions of low-valent cations (Fe^{2+} or Mg^{2+}) toward high ones (Si^{4+} or Al^{3+}) (Tombácz and Szekeres, 2006), But the edges show a pH-dependent charge as the extended discontinuity of Si–Al bonds (Zhou et al., 2012). As the consequence, when pH < $pH_{pzc,\ edge}$, surface protonation endows the edge with positive charges, and at pH > $pH_{pzc,\ edge}$, deprotonation brings it with negative one (Fig. 2c). The charges are usually measured negative at a low IS. It may result from that fewer positively charged (+) sites than negative (−) ones, and that the sites on edges can be screened by the spillover of the diffuse double layer from the facets (Tang et al., 2018; Sabaraya et al., 2021). Kl has the similar phenomenon with Mt, except that its Al–OH facets carry positive charges at pH < $pH_{pzc,\ edge}$ (Fig. 2d). This differentiation may come from its fewer displaceable isomorphic sites and less permanent structural charges (Sabaraya et al., 2021).

2.2. Iron (hydr)oxides

The iron (hydr)oxides, mainly including hematite, goethite, magnetite and ferrihydrite, possess their own specific morphology (Fig. 2e) and pH_{PZC} (Table 1). They are formed by oxidization and hydration, vitally affecting the fate and transport of pollutants (Tang and Lo, 2013; Li et al., 2020b; Wu et al., 2022).

Hematite (α-Fe_2O_3) is one of the most abundant and stable iron oxides with spherical or spheroidal shapes. With $-OH_2^+$ surface functional groups, hematite nanoparticles (HemNPs) usually present positive potential (Huynh and Chen, 2014; Sheng et al., 2016b). Goethite (α-FeOOH) is the most thermodynamically stable crystalline iron oxyhydroxide (Liu et al., 2017). The de-/protonation of Fe–OH groups lead to the pH-dependent surface charges, which governs its behaviors (Zhu et al., 2019). Magnetite (γ-Fe_3O_4) is a ferromagnetic iron oxide with the apparent magnetic properties. The influence of its peculiar magnetic properties on aggregation is apparent under magnetic fields, where ferromagnetic or paramagnetic dispersions form chain-like aggregates (Phenrat et al., 2007). Ferrihydrite (Fh) is a poorly crystalline but ubiquitous iron hydroxide. Its pH_{PZC} is around 7, implying the instability in the natural environment and the constraint by solution chemistries (Liao et al., 2017; Li et al., 2020b).

2.3. Others

Suspend sediment (SS) is an essential component in the waters and presents plate-like sheets and large hydrodynamic diameters (Zhao et al., 2021a). It settles manufactured materials out via the heteroaggregation propensity with particles and the sedimentation in turbulent water (Velzeboer et al., 2014; Li et al., 2019). Comprising various inorganic components and substantial organic matters, it has quite heterogeneous size and chemical content. Besides, no pH_{PZC} can be determined and negative potential is permanently maintained (Zhao et al., 2021a), but a higher heteroaggregation rate with ENPs than other NICs was observed (Velzeboer et al., 2014).

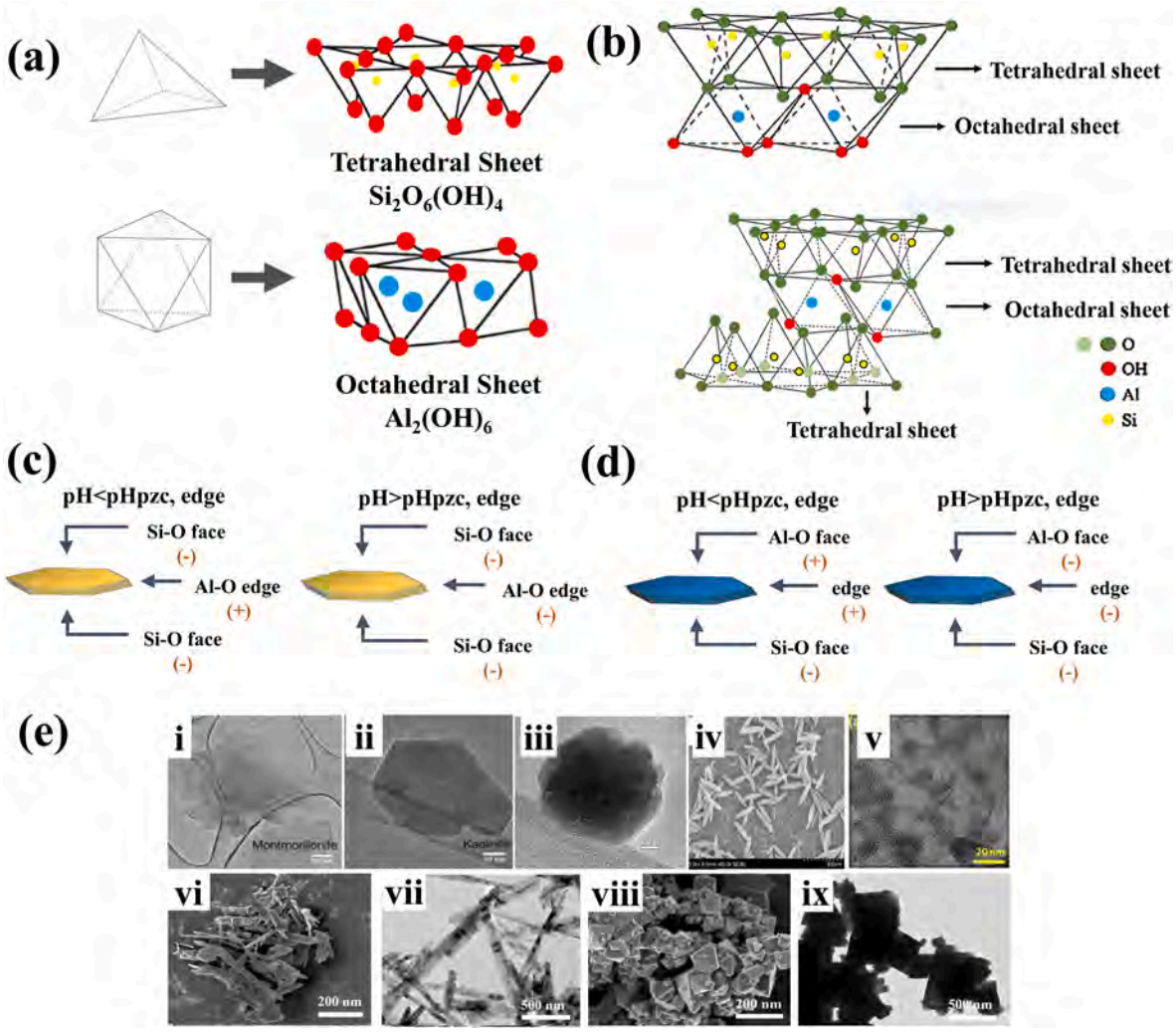

Fig. 2. (a) The constituent layers of clay mineral. The SiO_4^{2-} tetrahedra make up the tetrahedral sheets, the yellow filled circles represent silicon atoms and red filled circles represent hydroxyl groups. Octahedron constitutes the Octahedral sheets, blue filled circles represent metal centers and red filled circles represent hydroxyl groups (Uddin, 2017); (Awad et al., 2019). (b) The kaolinite and montmorillonite structure (Awad et al., 2019). (c–d) The simplified image of (c) montmorillonite and (d) kaolinite charge heterogeneity (Hu et al., 2020). (e) The SEM of (i) montmorillonite and (ii) kaolinite (Sabaraya et al., 2021). (iii) High-resolution TEM of HemNPs (Huynh et al., 2012); (iv) SEM image of spheroidal hematite particles of 4.7 ± 0.7 aspect ratio (Upendar et al., 2018); (v) TEM images of pristine ferrihydrite NPs alone (Liao et al., 2017); (vi) SEM and (vii) TEM images of goethite (Zhang et al., 2020); (viii) SEM and (ix) TEM images of magnetite (Zhang et al., 2020). All images are reproduced with permission. (For interpretation of the references to colour in this figure legend, the reader is referred to the Web version of this article.)

3. The environmental behaviors of NICs

The aggregation kinetics is related to particle collision frequency (K) and attachment efficiency (α). K is the probability of particles contacting with each other and α is a key parameter to quantify attaching probability. The equation, $k = K \times \alpha$ expressed the aggregation kinetics under ideal conditions (Quik et al., 2014). Therein, k, the apparent aggregation rate constant, is obtained from (Xu et al., 2015a):

$$\left(\frac{dD_h(t)}{dt}\right)_{t\to 0} \propto N_0 k \tag{1}$$

where D_h, the average hydrodynamic diameter; t, time; N_0, the initial particle concentration.

The attachment efficiency, α, is the inverse stability ration (1/W):

$$\alpha = \frac{1}{W} = \frac{k}{k_{fast}} = \frac{\frac{1}{N_0}\left(\frac{dD_h(t)}{dt}\right)_{t\to 0}}{\frac{1}{(N_0)_{fast}}\left(\frac{dD_h(t)}{dt}\right)_{t\to 0,fast}} \tag{2}$$

where the term "fast" refers to the favorable conditions.

When α is very small (~0), corresponding to that k is approximate zero, the particles will not aggregate. Then, as α increases ($0 < \alpha < 1$), partial aggregation takes place due to critical collisions and the declined interaction energy barrier. In this stage, called slow-aggregation stage or reaction-limited aggregation (RLA), colloidal stability could be affected by water chemistry. As α climbs continuously ($\alpha = 1$), a completely destabilized suspension is produced. This aggregation process reaches fast-aggregation stage or diffusion-limited aggregation (DLA), where the aggregation rates achieve the maximum (Wang et al., 2019b). The electrolyte concentration corresponding to RLA and DLA mutation points is critical coagulation concentration (CCC), that is a basic parameter to characterize the stability of nanoparticles in the dispersed system (Table 1). Additionally, it is closely associated with the electrolyte valence (Petosa et al., 2010):

$$CCC \propto \frac{1}{z^6 A_H^2} \tanh^4\left(\frac{ze\xi}{4k_B T}\right) \tag{3}$$

where A_H, the Hamaker constant; z, the ion valence; k_B, the Boltzmann

constant, 1.38×10^{-23} J K^{-1}; T, temperature; ξ, zeta potential.

When ξ is high (i.e., $\frac{ze\xi}{4k_BT} \gg 1$), the CCC is proportional to z^{-6}, known as Schulze-Hardy rule. On the contrary, when the potential is low (i.e., $\frac{ze\xi}{4k_BT} \ll 1$), the CCC is proportional to z^{-2}. As a result, the z-dependent CCC for most NPs should range from z^{-6} to z^{-2} (Petosa et al., 2010).

3.1. NICs homoaggregation

Homoaggregation behavior is essential and universal for NICs in the aqueous environment (Sharma et al., 2015). It can be constrained by physicochemical properties, influencing the fate and toxicity of pollutants, nutrient and pathogen (Lin et al., 2018; Sun et al., 2020b).

The platelet geometry and charge heterogeneity lead to an increased polarizability vector that appears across the basal plane for clay minerals. Self-association between clay particles may thus occur by face-to-face (F–F), edge-to-face (E−F), edge-to-edge (E−E). At pH < $pH_{PZC, edge}$, there is barrier-less E−F homoaggregation due to attractive forces between edges (+) and facets (−). When suspension pH > $pH_{PZC, edge}$, all surfaces are negatively charged. Therefore, E−F aggregation is no longer favorable and CCC are increased correspondingly (Fig. S1). Meanwhile, F–F and E−E aggregation are in low likelihood for clay platelet. As another main constituent of NICs, iron (hydr)oxides behave differently due to charge properties and different structure. With the increased salt concentration, the aggregation behaviors of HemNPs and goethite went through the stage from RLA to DLA (Chen et al., 2006; Huynh et al., 2012; Xu et al., 2015a). Magnetite NPs are unstable under the natural conditions. Its Fe–OH functional groups can be de-/protonated to $FeOH_2^+$ or $Fe–O^-$ under acidic and alkaline, respectively, which induced electrostatic repulsion to stabilize dispersion (Wang et al., 2017). Although the homoaggregation of NICs is of great importance, the existing articles are distinctly insufficient.

3.2. Heteroaggregation and sedimentation

With the intense human activities, huge numbers of ENPs have been discharged into the ecosystem. Carbon-based nanomaterials, exogeneous metal (oxides) and other emerging nanomaterials came into public light. With high mobility and reactivity, they might interact with the abundant NICs (Table 2).

3.2.1. Carbon-based materials

Carbon-based materials (CBMs), such as Graphene oxide (GO), fullerenes (C_{60}), carbon nanotubes (CNTs) and biochar, are increasingly used in industrial production and human life due to high absorption capacity, amphiphilicity, electrical conductivities and so on (Yi and Chen, 2013; Zhao et al., 2015; Shao et al., 2021). They are usually highly negatively charged, meaning the long-term stability (Zhao et al., 2015). However, this stabilization might be broken up when aggregating with omnipresent minerals, which is related to the solution pH and the abundant particle species.

At a higher pH, negatively charged CBMs and NICs were dominated by electrostatic repulsion (Sotirelis and Chrysikopoulos, 2017). Under lower pH conditions, iron (hydr)oxides and partial surfaces of clay minerals are positively charged. The generated electrostatic attraction between them induced a fast heteroaggregation (Sotirelis and Chrysikopoulos, 2017; Guo et al., 2020). Besides, no matter the acidity or alkalinity, some NICs can aggregate with CBMs through special interactions, like magnetic forces and bridging effect (Huynh et al., 2012; Ghosh et al., 2016; Huang et al., 2016; Feng et al., 2017).

The effects of different types of nanocarbon on the heteroaggregation behaviors of NICs-CBMs showed different characteristics (Fig. S2). For instance, due to the high hydrophobicity of fullerenes, they can be adsorbed on clays, thus triggering steric stabilization to inhibit secondary heteroaggregation (Guo et al., 2020). As compared, the peanut shells-derived biochars that produced at 300 and 600 °C had no interaction with clays, but could aggregate with iron hydr (oxides) via EDL attraction, especially the biochar at 600 °C (Liu et al., 2018a). For biochar colloids produced from different substance, Kl and goethite presented different behavior mechanisms in associating with them. Kl (+) increased the stability of the colloids by increasing electrostatic repulsion or charge shielding. Meanwhile, goethite (−) prompted the aggregation of some colloids via charge neutralization, whereas restrained that of others by charge shielding (Gui et al., 2021). From these interactions, the stability of biochar in the soils might be enhanced by these minerals, which benefits the carbon sequestration and

Table 2
The summarizing of the interaction between NICs and NPs.

NPs	Classifications	NICs	Ref.
Carbon-base nanomaterials	GO	Montmorillonite	Zhao et al., (2015)
		Kaolinite	(Yang et al., 2013; Zhao et al., 2015; Sotirelis and Chrysikopoulos, 2017)
		HemNPs	(Yang et al., 2013; Feng et al., 2017, 2019)
		Goethite	Zhao et al., (2015)
		KGa	Huang et al., (2016)
	C_{60}	Kaolinite	Guo et al., (2020)
		γ-Fe_2O_3 and magnetite	Ghosh et al., (2014)
		Goethite	Ghosh et al., (2016)
	CNTs	Montmorillonite	(Han et al., 2008; Zhang et al., 2012)
		Kaolinite	(Han et al., 2008; Zhang et al., 2012)
		HemNPs	(Huynh et al., 2012; Huynh and Chen, 2014)
	Biochar	Kaolinite	(Yang et al., 2018; Gui et al., 2021)
		HemNPs	Liu et al., (2018b)
		Goethite	(Liu et al., 2018b; Lian et al., 2019; Gui et al., 2021)
Metal or metal oxide nanoparticles	nZVI	Kaolinite and Montmorillonite	Wang et al., (2019a)
	AgNPs	montmorillonite, illite	(Zhou et al., 2012; Liu et al., 2015)
		Kaolinite	(Wang et al., 2015b; Dong and Zhou, 2020)
		HemNPs	(Huynh et al., 2014; Huang et al., 2019)
		SS	Zhao et al., (2021a)
	TiO_2	Montmorillonite	(Zhou et al., 2012; Labille et al., 2015)
		Kaolinite	(Wang et al., 2015b; Guo et al., 2019)
Metal or metal oxide nanoparticles	CeO_2	Montmorillonite	Zhao et al., (2021b)
		Kaolinite	Zhao et al., (2021b)
		HemNPs	(Oriekhova and Stoll, 2019; Zhao et al., 2021b)
		Goethite	(Li et al., 2020a; Zhao et al., 2021b)
		SS	Lv et al., (2020)
	Cit-AuNPs	HemNPs	Smith et al., (2015)
	CuO, ZnO	Clay	(Gupta et al., 2017; Kansara et al., 2019; Parsai and Kumar, 2020)
	MnO_2	HemNPs, Goethite	Zhang et al., (2015)
Other specific materials	PSNPs	Montmorillonite, Kaolinite	(Singh et al., 2019; Zhang et al., 2020)
		HemNPs, Goethite	Zhang et al., (2020)
		SS	Li et al., (2019)
	MoS_2	Montmorillonite, Kaolinite	Sabaraya et al., (2021)
	Silica nanoparticles	HemNPs	Upendar et al., (2018)

greenhouse gas mitigation (Yang et al., 2018).

Different types of CBMs and NICs may form kinds of aggregate structures through various interactions, which influenced the results of aggregation. A multilayered structure of GO sheets is formed when aggregating with goethite, because charge neutralization lowers the interlayer repulsion between GO (Zhao et al., 2015). Fullerene could produce the closed-loop structure with goethite due to the head-tail magnetism, the orderly assembled one with pure magnetic iron oxides, and the dimensional structures (1D, 2D, 3D) in Kl-C_{60} heteroaggregates (Ghosh et al., 2014, 2016, 2019). These provided new insights into the transport of organo-mineral complexes in global carbon cycling. In conclusion, the questions that how other CBMs (e.g., reduced GO and activated carbon) interact with NICs, and whether we can modify them to weaken their negative impact on the environment, are still needed to explore further.

3.2.2. Metal (oxide) nanoparticles

As another large component of ENPs, metal (oxide) nanoparticles (MNPs), such as AgNPs, nanoparticulate zero-valent iron (nZVI), TiO_2, cerium oxide nanoparticles (CeO_2 NPs), have universe and inevitable interactions with NICs in water systems. Like CBMs, particle surface potential is of great importance in their interactions.

The material properties and solution pH can influence surface potential to control colloidal behavior. For example, positively charged and uncharged CeO_2 significantly destabilized Kl suspension by charge neutralization and/or shading. The negatively charged CeO_2 enhanced its colloidal stability by electrostatic repulsion (Fig. S3) (Guo et al., 2019). In acidic waters, the negatively charged AgNPs could adsorb onto the Al–O faces and edges of Kl, declining positive charges and inhibiting aggregation of KL. On the other hand, it could heteroaggregate intensively with Mt edge by electrostatic attraction due to the spillover of negative basal plane EDL (Zhou et al., 2012; Wang et al., 2015b). As for TiO_2 (+), it formed primary heteroaggregates with Kl via electrostatic attraction and then secondary heteroaggregates via bridging. In comparison, it heteroaggregated with Mt face to make the suspension unstable (Fig. 3) (Zhou et al., 2012; Wang et al., 2015b). Differently, at a higher pH, the clay minerals were more prone to interact with the positively charged MNPs via electrostatic attraction, while the edges were the main sites through VDW and Lewis acid-base interactions (Fig. S4) (Wang et al., 2019a). Amounts of MNPs could aggregate with clay minerals, but the interaction modes were still unclear (Kansara et al., 2019; Parsai and Kumar, 2020).

The positively charged iron (hydr)oxides have relatively explicit heteroaggregation manners compared with clay minerals. For instance, when comparing these NICs for CeO_2 (−), their aggregation capacity followed the sequence Mt > goethite > hematite > Kl, agreeing with the adsorption capacity and DLVO energy (Zhao et al., 2021b). Additionally, the iron (hydr)oxides aggregated with MNPs following the "electrostatic patch" mechanism because they are oppositely charged (Smith et al., 2015; Zhang et al., 2015). But in other cases, no aggregation was observed between CeO_2 NPs and Fe_2O_3 or goethite owing to the electrostatic repulsion (Oriekhova and Stoll, 2019; Li et al., 2020a). Concerning the interaction between AgNPs and HemNPs, they can not only keep stable due to the electrostatic and steric repulsion, but also quickly aggregate because of electrostatic attraction (Huynh et al., 2014; Huang et al., 2019). This difference might come from the synthesis methods and solution chemistries. More difference for various ENPs could be found out to understand their behaviors in the natural environment.

In terms of SS, its interaction with AgNPs is negligible due to their negative charges (Zhao et al., 2021a). But for CeO_2, SS prompted it through the strong adsorption capacity in all cases (Lv et al., 2020). Although many published particles have researched into ENPs and NICs, the knowledge gaps concerning their aggregation still existed.

3.2.3. Other emerging materials

Except what we mentioned above, some emerging nanoparticles (e.g., plastics, MoS_2) also interacted with NICs (Duan et al., 2021; Sabaraya et al., 2021). Global plastics production has reached almost 367 million tons in 2020. China produces 32% of the whole, ranking first in the world (PlasticsEurope, 2021). Micro- and nanoplastics are distributed anywhere through decomposition process (Liu et al., 2019b; Singh et al., 2019), which poses a high potential risk due to the small size and high surface area (Wang et al., 2021a). Thus, their interactions with NICs become critical and urgent to be known about. Two iron oxides have

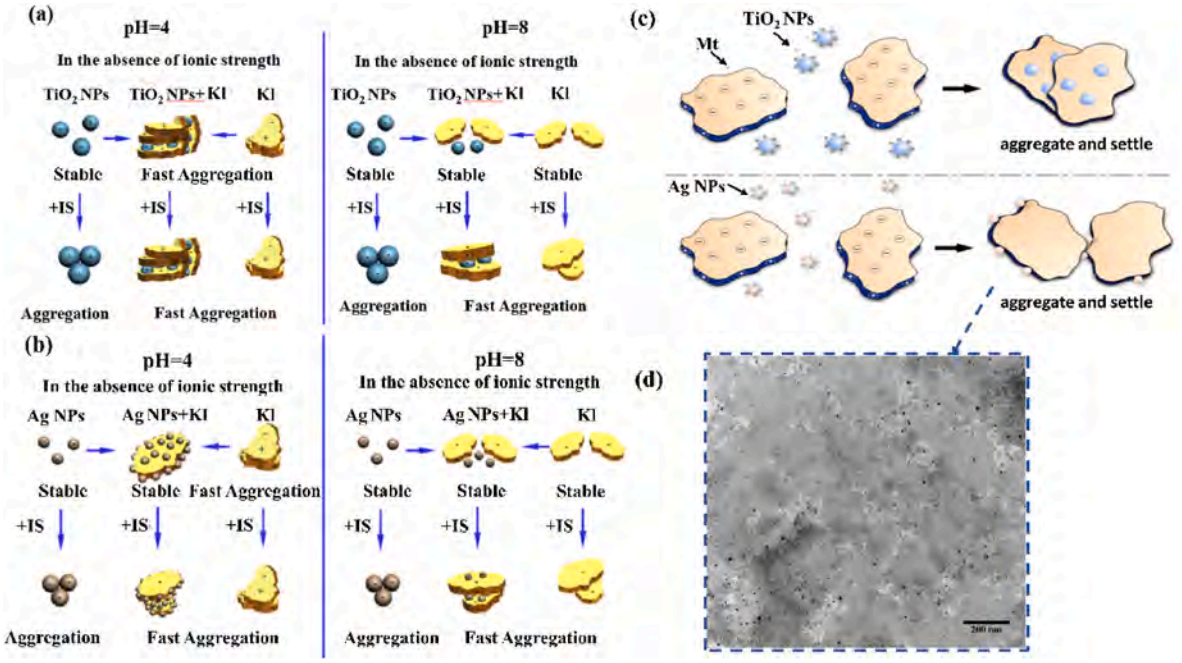

Fig. 3. The interaction between TiO_2 NPs or Ag NPs and Kl or Mt. The schematic description of heteroaggregation between (a) TiO_2 NPs and Kl, (b) Ag NPs and Kl. Reprinted with permission from (Wang et al., 2015b). Copyright (2015) Elsevier. (c) The schematic description of heteroaggregation between TiO_2 NPs or Ag NPs and Mt, and (d) the corresponding SEM of Ag NPs-Mt heteroaggregates (Zhou et al., 2012). Copyright (2015) Elsevier and (2012) American Chemical Society.

been reported to destabilize polystyrene nanoplastics (PSNPs) via strong electrostatic attraction and adsorption capacity (Fig. S5a) (Zhang et al., 2020). Further, the stabilization of PSNPs might be disturbed by Mt with IS increasing because of the transition from charge repulsion to neutralization (Singh et al., 2019; Zhang et al., 2020). This similar destabilization by the high IS might be ceased because the aggregation entered into DLA regime for the binary system containing PSNPs and large SS (Li et al., 2019). Conversely, the sedimentation of polyethylene microplastic was barely impacted by small SS owing to their low heteroaggregation tendency (Li et al., 2019).

Another emerging two-dimensional MoS_2 arose wide concern recently (Fig. S5b). At pH 4, MoS_2 can heteroaggregate with clay minerals via electrostatic interaction. The aggregation rate of MoS_2−Mt was higher than that of MoS_2−Kl; therein, the former interaction produced a loosely-bound structure (E–F aggregates) mainly through charge attraction, and the latter formed a compact one (F–F and E–F aggregates) because of the rigid nature of Kl. However, it did not appear under higher pH conditions due to the negative surface charge (Sabaraya et al., 2021).

3.3. Disaggregation

The disaggregation may occur by strong hydrodynamic forces and ultrasonic energy (Huynh and Chen, 2014). The CNTs-HemNPs heteroaggregates were disaggregated in an ultrasonic bath, then the aggregates regrow after ultrasonication. The elevated pH and additive NOM could also enhance the propensities of disaggregation. However, no re-aggregation would occur in the later cases (Baalousha, 2009; Huynh and Chen, 2014). For example, the GO-HemNPs aggregates broke down into small particles with increasing pH. The deprotonation of GO and the charge reversal of HemNPs resulted in their negative surface charges and the weakened GO−HemNPs bonds (Feng et al., 2019). High concentration of humic acid induced the disaggregation of iron oxides nanoparticles due to the enhanced electrostatic repulsion (Baalousha, 2009). The condition that disaggregation occurs might be miscellaneous but few studies explored, drawing us to investigate further.

Particle behaviors can scavenge the manufactured materials or stabilize the particle suspension. Large amounts of studies investigated basic interactions and novel analytical methods in complex water chemistries. Still, the behaviors of emerging materials need to be investigated further to control and lower risks. The behaviors in actual waters also make significant difference from laboratory experiment, which urges us to establish association between them.

4. Mechanisms and modelling of the behaviors

4.1. DLVO theory

The classical DLVO theory was used to explain the stability of nano- and micro-particles (Hotze et al., 2010). It was often employed in sphere−sphere (NP-NP), sphere−plate (NP-collector) and plate−plate (collector-collector) patterns (Table S2). According to DLVO theory, the net interaction energy between particles is the sum of VDW attraction and EDL repulsion, as a function of particle size, Hamaker constant (A_H), surface potential and solution chemistry (Phenrat et al., 2007).

The equation can be expressed as

$$V_{DLVO}(h) = V_{VDW}(h) + V_{EDL}(h) \tag{4}$$

where V_{DLVO}, V_{VDW} and V_{EDL} denote the total, van der Waals and electrostatic interaction energy, respectively; h, the distance between materials.

VDW attraction contains the Keesom (or orientation) force, the Debye induction force and the London (or dispersion) force. Its strength strongly depends on A_H, a value relating to NPs properties (Chen et al., 2016). The higher A_H means the greater aggregation tendency for particles (Hotze et al., 2010). The relation between particles and medium expressed in the following

$$A_{121} = \left(A_{22}^{1/2} - A_{11}^{1/2}\right)^2 \tag{5}$$

$$A_{123} = \left(A_{22}^{1/2} - A_{11}^{1/2}\right)\left(A_{22}^{1/2} - A_{11}^{1/2}\right) \tag{6}$$

where A_{11}, A_{22}, and A_{33} denoted A_H of NPs “1”, medium, NPs “2” in vacuum, respectively; A_{121} and A_{123} denoted the Hamaker constants for homoaggregation between NPs “1” and heteroaggregation between NPs “1” and “2”, respectively.

The mathematics of EDL force is based on the assumption that with the distance increasing, the alteration of particle surface charges follows the Poisson-Boltzmann distribution. The electrostatic force decreases exponentially with distance and can be easily affected by IS. The Debye length (κ) is the inverse of EDL thickness, and

$$\kappa = \sqrt{\frac{1000e^2}{\varepsilon KT}\sum_i z_i M_i} \tag{7}$$

where M_i is molar concentration of electrolyte.

Hence, when the solution IS increases, the thickness of the double layer reduces, which decreases the electrostatic repulsion and facilitates aggregation(Grasso et al., 2002).

4.2. DLVO interaction energy profiles

As the separation between two particles increases, the VDW attraction inversely and EDL repulsion exponentially decreases, respectively. Specifically, as particles get close, the interparticle DLVO energy might go through a weak secondary minimum (a shallow attractive well), an energy barrier and a primary minimum (a deep attractive well). The reversible aggregation usually exists in the secondary minimum and only when the interaction energy overpasses the barrier, the primary minimum can be arrived (Islam et al., 1995; Buffle et al., 1998). Three main situations exist in the DLVO energy of particle aggregation (Fig. S6).

4.3. X-DLVO

The X-DLVO theory also plays a vital role in speculating the fate and transport of particles, such as H-bonding, Lewis acid-base (AB) force, steric interaction, bridging and so on (Fig. 4). These interactions are proposed in different specifical cases, needing to discuss and analyze in detail.

4.3.1. H-bonding

As we all know, high electronegative atoms have the propensity to despoil electron from proton to form H-bonding (Grasso et al., 2002). It often appears between colloids or the nanoparticles with substantial oxygen-containing groups, and between the modified NPs and hydrated ions (Wang et al., 2015a, 2017; Chen et al., 2017). Its strength will be weakened when pH is far from the neutral. Specifically, having the hydroxyl moieties, goethite was likely to associate with other NPs (e.g., CDs, nano-black carbon and PSNPs) to facilitate aggregation (Liu et al., 2017; Lian et al., 2019; Zhang et al., 2020). However, H-bonding formed between silanols and hydroxyls of clay surface may be the culprit for the decreased aggregation (Sun et al., 2021c).

4.3.2. Lewis acid-base force

Lewis acid-base (AB) force, defined as the acceptor-donor interactions between electrons, is the driving force for hydrophilic repulsion and hydrophobic attraction (van Oss, 1993). It exists between an “unshielded” proton (Lewis acid, electron acceptor/proton donor) and available electrons (Lewis base, electron donor/proton acceptor)

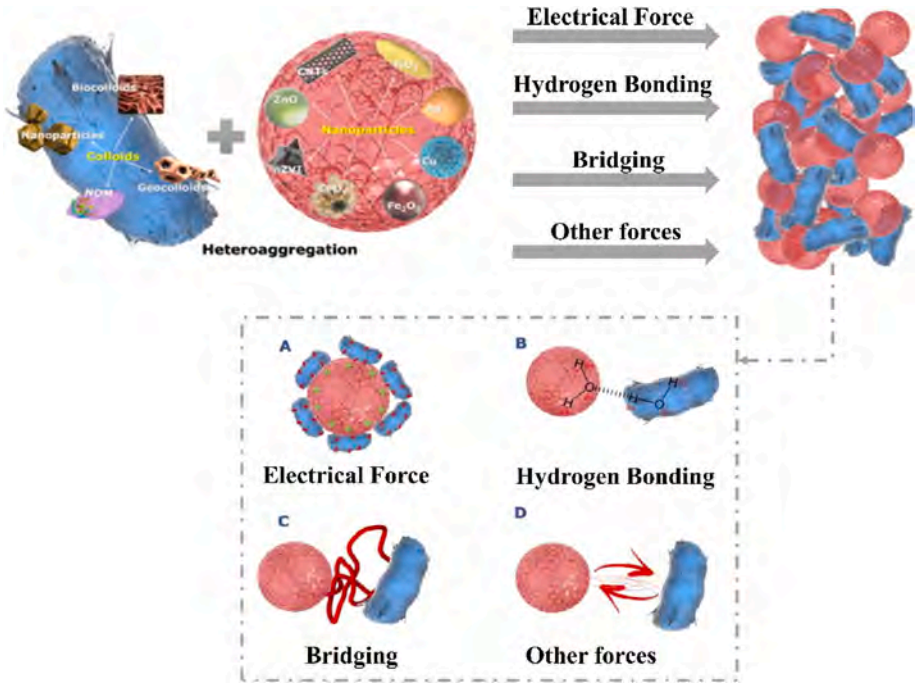

Fig. 4. The schematic description of the interactions between NICs and nanoparticles. Reproduced from (Wang et al., 2015a). Copyright (2015) Elsevier.

(Grasso et al., 2002). Its strength will decrease with increasing pH (Yang et al., 2013). The AB interaction is a short-range force (Hermansson, 1999), and can be calculated from (Hotze et al., 2010):

$$\frac{V_{AB}}{\text{Surface area}} = \Delta G_{H_0}^{AB} \exp\left(\frac{H_0 - H}{\lambda}\right) \tag{8}$$

where, $\Delta G_{H_0}^{AB}$, free energy of AB interaction between particles at distance H_0; H_0, minimum equilibrium separation distance; H, the distance between the two particle surfaces; λ, decay length for AB interactions.

Lewis AB force can promote aggregation for particles. For instance, in the scenario of goethite (Lewis base) and carbon dots or black carbon (Lewis acids), it may overcome the charge repulsion and conduce to the adsorption between them (Liu et al., 2017; Lian et al., 2019). Furthermore, AB force, rather than the classical DLVO theory, is suitable for rough surfaces (Hoek and Agarwal, 2006).

4.3.3. Steric interaction

Commonly, steric interaction enhanced colloidal stability when polymer or polyelectrolyte is adsorbed or grafted onto particle surfaces (Chen et al., 2010; Shrestha et al., 2020). However, the particle fullerene also could adsorb onto kaolinite surface to provide the increased steric hindrance (Guo et al., 2020). It often integrally linked with electrostatic repulsion, making up the electrosteric stabilization, but the total interaction energy cannot be easily summed up (Romero-Cano et al., 2001; Fritz et al., 2002). The electrosteric stabilization can be affected by solvent chemistries, while steric force was influenced by polymer properties (surface density, molecular weight and solubility of the portion extending into solution) (Fritz et al., 2002; Chen et al., 2010). The adsorbed mass, layer thickness and conformational changes of the adsorbed NOM might also have impacts (Li et al., 2020b; Ding et al., 2021).

The steric force has two contributions: osmotic and coil compression. Thermodynamically, the compression equals to a configurational entropy net loss. An osmotic effect V_{Osm} will generate when the distance between two particles is twice smaller or equal to the thickness of adsorbed layer.

$$\frac{V_{Osm}}{k_B T} = 0 \quad 2L \le H \tag{9}$$

$$\frac{V_{Osm}}{k_B T} = \frac{4\pi a}{v_1}\varphi_P^2\left(\frac{1}{2} - \chi\right)\left(L - \frac{H}{2}\right)^2 \quad L \le H < 2L \tag{10}$$

$$\frac{V_{Osm}}{k_B T} = \frac{4\pi r}{v_1}\varphi_P^2\left(\frac{1}{2} - \chi\right)L^2\left[\frac{H}{2L} - \frac{1}{4} - \ln\left(\frac{H}{L}\right)\right] \quad L > H \tag{11}$$

where r, the particle radius; χ, the Flory-Huggins solvency parameter; φ_P, the volume fraction of polymer within the brush layer; L, the thickness of the brush; v_1, the volume of one solvent molecule.

When the distance is smaller or equal to the thickness, the elastic compression of the layer occurs, there, an entropy elastic repulsion V_{VR} comes into being.

$$\frac{V_{VR}}{k_B T} = 0 \quad L \le H \tag{12}$$

$$\frac{V_{VR}}{k_B T} = \left(\frac{2\pi r}{M_W}\varphi_P L^2 \rho_P\right)\left\{\frac{H}{L}\ln\left[\frac{H}{L}\left(\frac{3 - \frac{H}{L}}{2}\right)^2\right]\right\} - 6\ln\left(\frac{3 - \frac{H}{L}}{2}\right) + 3\left(1 + \frac{H}{L}\right) \quad L > H \tag{13}$$

where M_W, the molecular weight of the polymer; ρ_P, its density.

Substantial studies have found steric force takes an important role in stabilizing suspension in the presence of NOM (Huynh et al., 2012; Feng et al., 2019; Wang et al., 2019a). When the polymer that adsorbed onto particles surface unfolded, the increased conformational entropy resulted in the weakened steric force. Inversely, the suppressed or folded polymer leads to a lower entropy and the elevated steric hindrance (Fig. S7).

4.3.4. Bridging

Bridging, a molecular connection between two or more particles, leads to morphologically specific aggregation (Philippe and Schaumann, 2014). A basic requirement for bridging is enough unoccupied sites on

the particle surface where cation, polymer and NPs can adsorb onto and connect with other particles (Han et al., 2008; Huynh et al., 2012; Yang et al., 2018; Wang et al., 2019a).

Cation bridging is mainly found in suspension with Ca^{2+} or Mg^{2+} (Chekli et al., 2013; Tang et al., 2018; Oriekhova and Stoll, 2019). It could decrease suspension CCC and enhance aggregation because Ca^{2+} was adsorbed onto the surface through cation bridging and screening effect (Li et al., 2020a). Generally, the investigations concerning Mg^{2+} are scarcer than that about Ca^{2+} and even cannot be observed in some published articles (Chowdhury et al., 2013; Wang et al., 2017). But it might appear in the high Mg^{2+} concentration or in the presence of organic matters (Zhang et al., 2013; Tang et al., 2018). The bridging of trivalent cations (Al^{3+}, Fe^{3+}) was also certified to be vital (Li and Sun, 2011; Cheng et al., 2020b), but their important impact on the aggregation of NICs was not taken much consideration.

Same as cation bridging, polymer and surfactants bridging also provided favorable conditions for particle aggregation, e.g., bridging macromolecules enhanced the homoaggregation of NICs or the heteroaggregation with ENPs (Chen et al., 2006; Han et al., 2008). Moreover, particles can serve as bridging agents to connect particles in some heterogeneous system (Praetorius et al., 2014; Sun and Zhou, 2014). In the meantime, there might be depletion force existing between particles, as discussed below.

4.3.5. Depletion force

Depletion force exists usually in the heterogenous system containing both large and small size particles, with weak or even no electrostatic interactions (Feng et al., 2021). When large spheres approach each other, the excluded volumes overlap. As a result, those small spheres enter into a larger available volume. Then the increased total entropy of the system generally produces a depletion attraction between large spheres. Another explanation for this attraction originates from osmotic effect (Marenduzzo et al., 2006). However, it is not always attractive, which is greatly determined by the volume fraction of small particles (Landman et al., 2021). The higher volume fraction develops the depletion repulsion, meaning the enhanced stability (Ghosh et al., 2014). Specifically, the α-FeOOH hard rods aggregated with fullerene under the low volume fraction of C_{60} via depletion attraction. Furthermore, the aggregates sizes slightly decreased with the increasing fraction of C_{60} due to the transition to depletion repulsion (Ghosh et al., 2016). The mechanisms between iron oxides and fullerene were in agreement with the above (Ghosh et al., 2014). Zhou et al. (2012) supposed that depletion attractive force possibly resulted in the aggregation between Mt and AgNPs, but the suspension stability at pH 8 overturned this conclusion.

4.3.6. Magnetic and born force

The magnetic force benefits the adhesion efficiency of magnetite and hematite with no predicted aggregation barrier (Phenrat et al., 2007; Hong et al., 2009). The calculation of magnetic force is rarely used since the low magnetism of hematite and limited application of magnetite:

$$V_M = \frac{-8\pi\mu_0 M_s^2 r^3}{9\left(\frac{H}{r}+2\right)^3} \tag{14}$$

where μ_0, the permeability of the vacuum; M_s, saturation magnetization.

Born repulsive forces is a short-range interaction originating from the interpenetration of electron clouds around the atoms of particles and a planar surface when their separation distance is less than 0.5 nm (Yi and Chen, 2013; Shen et al., 2014).

$$V_{Born}(H) = \frac{A_H \sigma^6}{7560}\left[\frac{8r+H}{(2r+H)^7} + \frac{6r-H}{H^7}\right] \tag{15}$$

where σ, the collision diameter, a typical experimentally derived value for σ, 0.5 nm.

The competition between these forces plays out like a tug-of-war and the suspension stability lies on the winner. The VDW and EDL interaction play the dominant role and guide the other forces. Several interactions may take no effect in some situations, but they also have the pivotal influence in others. Actually, these interactions are still limited in explaining the phenomena in natural waters and more parameters needs to be measured and determined. Future studies should focus more on the modelling and the contribution proportion of these interactions to discern the dominant force under the complex environmental conditions.

5. Factors

Existing in the natural environment, particles might undergo various fate and transport by intrinsic and extrinsic factors. The interesting stabilization or mobility for particles under different conditions arouse wide concerns.

5.1. Particle characteristics

Particle characteristics are fundamental factors for behaviors. Specifically, on the one hand, particles with smaller size have a higher A_H, which is beneficial to particles aggregation (Hotze et al., 2010; Xu et al., 2020). Moreover, small particles possess more atoms exposed onto their surfaces, which leads to high surface activity and energy, making particles tend to aggregate into stable clusters (Shrestha et al., 2020). On the other hand, the smaller particle has the thicker EDL or structural hydration layer, which resulted into the resistance to aggregation (Sheng et al., 2016a; Sun et al., 2021b). This difference might come from the initial particle concentration.

Some non-spherical NICs have charge heterogeneity (Zhou et al., 2012; Wang et al., 2015b) and even form the special aggregates morphology (Lian et al., 2019). For instance, the well-crystallized and poorly-crystallized Kl have different aggregation tendencies and mechanisms (Wang et al., 2015b). As for the well crystallized low aspect (L_{Asp}) and the weakly crystallized high aspect (H_{Asp}) α-FeOOH, the latter has inherent crystal deficiencies and many surface charges, prompting its aggregation with fullerene via strong EDL attraction in acidic solution (Ghosh et al., 2016).

5.2. Particle concentration (ratio)

Particle concentration (ratio) affects collision efficiency, hence influencing particle aggregation (Shrestha et al., 2020). The mean surface distance between particles can be calculated through Woodcock's equation:

$$h_{susp} = D_p\left[\{1/(3\pi F) + 5/6\}^{0.5}\right] \tag{16}$$

where F, the solid fraction and D_p, the particle diameter.

As for the suspension of 300 nm particles, when the concentration exceeds 40 vol%, the h_{susp} is around 10 nm, then the EDL repulsion force alone is not adequate to stabilize suspension. At 10 vol%, the h_{susp} significantly exceeds 10 nm, consequently stabilizing the suspension is possible (Shrestha et al., 2020).

The effect of mass/number concentration ratio was mostly investigated on the particle stabilization (Labille et al., 2015). The plot of mass concentration ratio vs heteroaggregation rate exhibited a typical inverted "V" (Fig. 5) (Huynh et al., 2012). Lots of particles collided and attached into primary aggregates via electrostatic interaction and then aggregated into large clusters via particle bridging. As the ratio increased until the optimal value, the highest aggregation rate was reached, where the surface charges of particles were close to zero (Feng et al., 2017, 2019). Further, at the higher ratio, stable nanohybrids were formed owing to charge screening and reversal (Feng et al., 2017).

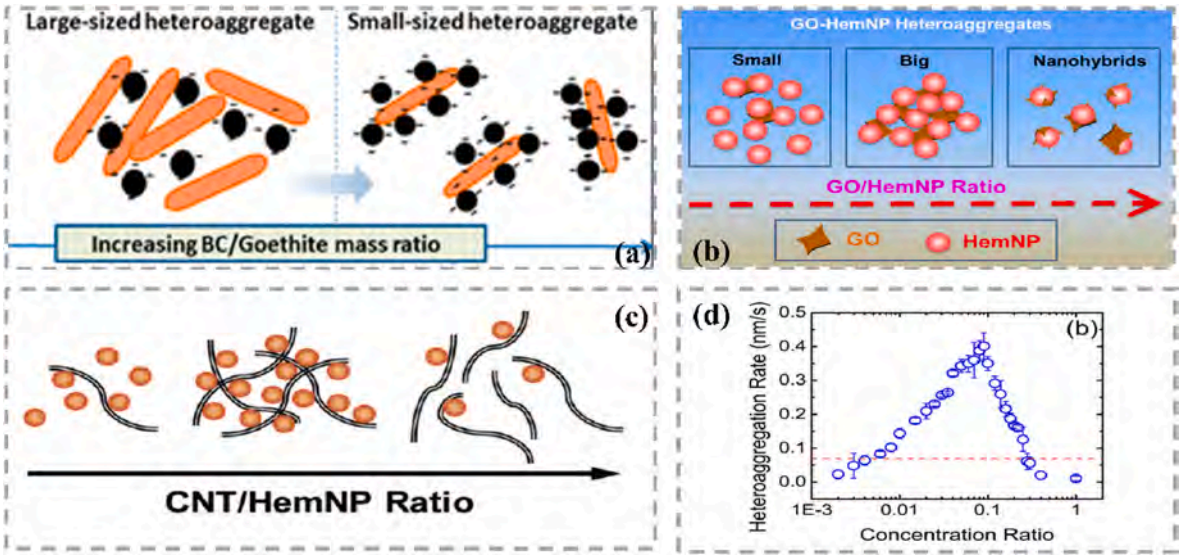

Fig. 5. The proposed heteroaggregation mechanisms at different mass concentration ratios. (a) The interaction between black carbon nanoparticles and goethite with increasing mass ratios (Lian et al., 2019); (b) the GO-HemNPs heteroaggregation with increasing GO/HemNP mass concentration ratios (Feng et al., 2017); (c) the heteroaggregation between CNT and HemNP (Huynh et al., 2012); (d) the heteroaggregation rates of NPs and NICs as a function of mass concentration ratio (Feng et al., 2017). Figures are adapted from references mentioned above with permission.

However, the decreasing phase was not found in nZVI−clay heteroaggregation. Their aggregation rate increased continuously as the concentration ratio due to the magnetic force of nZVI and bridging with clays (Wang et al., 2019a). This indicates that the suitability of this inverted "V" rule under NPs/NICs concentration ratios for various systems needs to explore further. Therefore, the fate and behavior of the final formed composite NPs might have vital environmental impacts, which should be paid attention to.

5.3. Solution pH and ionic strength

Solution pH has a profound effect on particle surface charges. When suspension pH approaches the particles pH_{PZC}, there is a rapid aggregation because of the decreased electrostatic repulsion (Zhu et al., 2014). At low IS, the farther the pH is from pH_{PZC}, the more stable the solution is (Xu et al., 2015b; Wang et al., 2019a). This may contribute to that pH can induce de-/protonation of the surface functional groups to change the sign of particle surface charge (Liu et al., 2018c; Guo et al., 2020).

As for ions, besides the aforementioned cation bridging, the high ionic concentration and valence in a certain range can reduce interparticle electrostatic repulsion extremely through the EDL compression or charge neutralization (Hotze et al., 2010; Lowry et al., 2012). For example, the capability of counter ions to enhance Kl aggregation is in the order of $Eu^{3+} > Sr^{2+} > Mg^{2+} > Cs^{+} > Na^{+}$ (Sun et al., 2020b). The anions destabilization for HemNPs and goethite NPs (+) followed the order: $NO_3^- \approx Cl^- < F^- < SO_4^{2-}$ (Xu et al., 2015b). Moreover, solution pH and ion concentration may impact the surface charge of particle, then affect the destabilization capacity of ions. For instance, at pH 9, the cations facilitated magnetite (−) aggregation by the decreased energy barrier, and the destabilization effects followed $Ba^{2+} > Sr^{2+} > Ca^{2+} > Mg^{2+} > Na^{+}$. In comparison, the magnetite particle charge presented positive at pH 5; therefore, the totally converse order was determined (Wang et al., 2017). As for the stability of goethite, its CCC of NaCl, $NaNO_3$, Na_2SO_4 were corresponded to the Schulze-Hardy rule but no CCC could be found for Na_3PO_4. When Na_3PO_4 concentration ranged from 0 to 1 mM, the aggregation rate increased firstly and then decreased because the goethite surface charge was neutralized followed by reversed. When the concentration continually increased, the amount of negative charges decreased because of the charge screening caused by sodium counter ions, which enhanced particle aggregation (Lin et al., 2018).

A number of studies focused on the effect of ions on the aggregation of particles carrying the opposite charges. However, the aggregation of particle in the presence of the ions with the same charge sign is also important. The mean aggregation rate for goethite (+) followed $Cu^{2+} < Ca^{2+} < Mg^{2+}$, because Cu^{2+} can substitute the atoms H and develop the strongest covalent bonding $-OCu^{+}$ to elevate activation energy, thus enhancing electrostatic repulsion. The anions also can affect the stability of cit-magnetite nanoparticles (−) and the sequence followed $PO_4^{3-} > SO_4^{2-} > Cl^-$, because PO_4^{3-} can be strongly adsorbed (Liu et al., 2018c).

5.4. NOM

NOM, consisting of humic substances (HS) and non-humic ones (NHS), interact with NPs through their surface oxygen-containing functional groups (Grillo et al., 2015; Artifon et al., 2019; Junaid and Wang, 2021). Their interaction can be inhibited by changing particle surface charge and inducing interparticle steric stabilization (Chen et al., 2017; Barbero et al., 2021), or be enhanced by charge neutralization, bridging and others (Fig. S8) (Hu et al., 2010a; Sun et al., 2018). These interactions might also affect the transport and reactivity of NOM in turn and other transformation and reaction process in the environment.

On the one hand, NOM induced colloidal stabilization. HS and small molecular acids can be adsorbed to clay edges through ligand exchange to stabilize suspensions (Heidmann et al., 2005; Guo et al., 2020). Meanwhile, protein (Feng et al., 2019; Yan et al., 2019; Sun et al., 2022) and extracellular polymeric substance (Lin et al., 2018; Wang et al., 2018b; Zhao et al., 2021b) can coat NP surfaces to enhance electrostatic or steric repulsion. On the other hand, the aggregation induced by NOM also existed. For instance, alginate can bridge with Ca^{2+} or particles to form alginate gels (Chen et al., 2006; Wang et al., 2018a). The negatively charged NOM can also interact with positively charged NPs through EDL attraction (Palomino and Stoll, 2013a; Sheng et al., 2016b). The studies concerning the effect of NOM on particle aggregation have been largely comprehensive, but the ones focusing on the heteroaggregation of NICs-ENPs are relatively rare.

These (de)stabilization might depend on the type and concentration of NOM and the electrokinetic properties of NPs. For instance, compared

to fulvic acid (FA), the abundant reactive groups of humic acid (HA) made it possess stronger adsorption capacity, thus the HA-induced aggregation was more dependent on water chemistry (Weng et al., 2007). Although both HA and FA inhibited Fh NPs aggregation, CH_3COONa did not (Liu et al., 2019a). Furthermore, when NOM concentration was low, the enhanced Fe oxides homoaggregation and the weakened Fe oxides-MnO_2 heteroaggregation occurred due to the oppositely charged patches. With the increased NOM concentration, heteroaggregation were thwarted because all particles were negatively charged (Hu et al., 2010a; Zhang et al., 2015). It even led to disaggregation originating from EDL repulsion, VDW forces and hydrophobic forces (Palomino and Stoll, 2013b). As for alginate bridging, it was not observed in the association between CeO_2 NPs and Fe_2O_3 NPs. Low concentration of alginate had no effect, while high one inhibited the heteroaggregation due to electrostatic interaction rather than bridging (Oriekhova and Stoll, 2019). In addition, the adsorption mass and conformation change of macromolecules might alter the surface charge and adsorbed layer thickness of NICs, thus influencing electrostatic interaction and steric repulsion.

The environmental factors are also important in determining the impacts of NOM. For instance, the increased pH made the less electrostatic repulsion between NOM and clays, and then the hydrophobic or H-bonding interactions began to take effect (Sabaraya et al., 2021). High concentration of multivalent cations led to the stabilization of NOM-coated particles through the decreased attractive interaction and the increased steric force, while the low one induced fast aggregation by patched charge attraction (Sheng et al., 2016b). This study focused on the stabilization of the secondary aggregates to provide a new perspective on particle aggregation. Moreover, the different exposure orders of electrolyte with high concentrations and protein was also found to have a significant role in the aggregation of HemNPs (Ding et al., 2021). Except the aforementioned, more environmental factors in the natural waters are urgent to be revealed and to be investigated in aggregation experiment to simulate real water systems and solve the actual environment problems.

6. Conclusions and environmental implications

This article comprehensively reviewed NICs behavior in the water system. They can not only homoaggregate with themselves, but also heteroaggregate with carbon-base colloids, metal (oxide) colloids and other emerging colloids. To explain and predict these behaviors, the associated mechanisms and modelling (DLVO and X-DLVO theory) were proposed. The classical DLVO theory was usually employed in ideal situations, and the X-DLVO theory was developed in terms of non-ideal conditions, which provided new perspectives on particle behaviors. Additionally, a variety of intrinsic and extrinsic factors were proposed to explore the generality and speciality of particle behaviors. Their interactions are mutually connected, therefore taking a diversity of factors into consideration simultaneously is important and necessary.

Despite of many studies in this field, there still exist some problems and gaps that need to be settled out and investigated further.

(i) Pay more attention to the emerging materials. Except the traditional CBMs and MNPs, some new matters have unpredictable risks affecting the stability and eco-balance of the nature, such as 2D-nanomaterials (e.g., Cofs, mofs, Mxene), the nanoporous materials, transition metal dichalcogenides and phase change materials. They may present different physicochemical characteristics, thus interacting with NICs via peculiar mechanisms in the waters. It probably gives us novel inspiration on understanding particle behaviors and fates and on controlling potential environmental risks in aquatic system.

(ii) Innovate the detecting and analytical methods systematically. For example, the low concentration of NPs might make them unmeasurable in most cases. In addition, it is difficult to observe *in situ* the changes in particle size and morphology during aggregation, the absorption content and thickness of NOM on the particles, and the structural changes when NOM interacts with NPs by current techniques. Thus, some analytical apparatus can be combined together to determine them accurately and timely.

(iii) Numerical analytic and methodological models should be further developed. Particle homoaggregation has been explored thoroughly, albeit for the more complex heteroaggregation, there exists the deficiency in numerical models yet. It is worth noting that artificial intelligence and machine learning models are applied broadly with the arrival of information evolution. Huge development potential exists in this area, therefore incorporating the latest and traditional technologies might open up new sights in evaluating pollution fate and transport.

(iv) How to combine micro experimental phenomena with macro environmental problems has become a vital development direction in the future. Considering the environmental complexity, it is expected that operating *in situ* observation and particle size measuring on the spot support the knowledge about natural situation. The existing factors that we talked are not adequate to clarify particles behavior in the natural environment. Lots of factors need us to explore in the natural environment, such as the temperature, the concentration of nutrients and pollutants, the emerging organic or inorganic materials, as well as the interaction zones, where the particles might experience the dramatic change of environmental conditions.

Future studies can focus more on these aspects and discuss relative mechanisms to offer novel insights. With more and more pollutants putting into the environment, the development of the investigation on NICs behaviors will continue as before. We anticipate that more intensive research could focus on solving the technical and theoretical problems concerning pollutants-control and overcoming the current constraints in environmental applications.

Credit author statement

Yihui Guo: Methodology, Analysis, Writing-Original Draft and Review, Ning Tang: Methodology, Writing-review and editing, Jiayin Guo: Analysis, Review and editing, Lan Lu: Review and editing, Na Li: Review and editing, Tingting Hu: Review and editing, Ziqian Zhu: Review and editing, Xiang Gao: Review and editing, Xiaodong Li: Methodology, Review and editing, Longbo Jiang: Methodology, Review and editing, Jie Liang: Supervision, Methodology, Analysis, Review and editing.

Declaration of competing interest

The authors declare that they have no known competing financial interests or personal relationships that could have appeared to influence the work reported in this paper.

Data availability

No data was used for the research described in the article.

Acknowledgments

This work was supported by the National Natural Science Foundation of China (51979101, 72088101, 51679082, 51479072, 51521006, 52170180), the Hunan Science & Technology Innovation Program (2018RS3037), and the Natural Science Foundation of Hunan Province (2019JJ20002).

Appendix A. Supplementary data

Supplementary data to this article can be found online at https://doi.

org/10.1016/j.chemosphere.2022.136805.

References

Abbas, Q., Yousaf, B., Ullah, H., Ali, M.U., Ok, Y.S., Rinklebe, J., 2020. Environmental transformation and nano-toxicity of engineered nano-particles (ENPs) in aquatic and terrestrial organisms. Crit. Rev. Environ. Sci. Technol. 50, 2523–2581.

Artifon, V., Zanardi-Lamardo, E., Fillmann, G., 2019. Aquatic organic matter: classification and interaction with organic microcontaminants. Sci. Total Environ. 649, 1620–1635.

Awad, A.M., Shaikh, S.M.R., Jalab, R., Gulied, M.H., Nasser, M.S., Benamor, A., Adham, S., 2019. Adsorption of organic pollutants by natural and modified clays: a comprehensive review. Separ. Purif. Technol. 228, 115719.

Baalousha, M., 2009. Aggregation and disaggregation of iron oxide nanoparticles: influence of particle concentration, pH and natural organic matter. Sci. Total Environ. 407, 2093–2101.

Bakshi, S., He, Z.L., Harris, W.G., 2015. Natural nanoparticles: implications for environment and human health. Crit. Rev. Environ. Sci. Technol. 45, 861–904.

Bansal, P., Deshpande, A.P., Basavaraj, M.G., 2017. Hetero-aggregation of oppositely charged nanoparticles. J. Colloid Interface Sci. 492, 92–100.

Barbero, F., Mayall, C., Drobne, D., Saiz-Poseu, J., Bastús, N.G., Puntes, V., 2021. Formation and evolution of the nanoparticle environmental corona: the case of Au and humic acid. Sci. Total Environ. 768, 144792.

Boström, M., Williams, D.R.M., Ninham, B.W., 2001. Specific ion effects: why DLVO theory fails for biology and colloid systems. Phys. Rev. Lett. 87, 168103.

Buffle, J., Wilkinson, K.J., Stoll, S., Filella, M., Zhang, J., 1998. A generalized description of aquatic colloidal interactions: the three-colloidal component approach. Environ. Sci. Technol. 32, 2887–2899.

Carstens, J.F., Bachmann, J., Guggenberger, G., 2021. Aggregation and transport behavior of goethite colloids as affected by dissolved organic matter and pH: electrostatic vs. hydrophilic interactions. Colloids Surfaces A Physicochem. Eng. Asp. 609, 125639.

Chekli, L., Phuntsho, S., Roy, M., Lombi, E., Donner, E., Shon, H.K., 2013. Assessing the aggregation behaviour of iron oxide nanoparticles under relevant environmental conditions using a multi-method approach. Water Res. 47, 4585–4599.

Chen, H., Koopal, L.K., Xiong, J., Avena, M., Tan, W., 2017. Mechanisms of soil humic acid adsorption onto montmorillonite and kaolinite. J. Colloid Interface Sci. 504, 457–467.

Chen, K.L., Mylon, S.E., Elimelech, M., 2006. Aggregation kinetics of alginate-coated hematite nanoparticles in monovalent and divalent electrolytes. Environ. Sci. Technol. 40, 1516–1523.

Chen, K.L., Smith, B.A., Ball, W.P., Fairbrother, D.H., 2010. Assessing the colloidal properties of engineered nanoparticles in water: case studies from fullerene C60 nanoparticles and carbon nanotubes. Environ. Chem. 7.

Chen, Q., Xu, S., Liu, Q., Masliyah, J., Xu, Z., 2016. QCM-D study of nanoparticle interactions. Adv. Colloid Interface Sci. 233, 94–114.

Cheng, H., Yang, T., Jiang, J., Lu, X., Wang, P., Ma, J., 2020a. Mn2+ effect on manganese oxides (MnOx) nanoparticles aggregation in solution: chemical adsorption and cation bridging. Environ. Pollut. 267, 115561.

Cheng, H., Yang, T., Ma, J., Jiang, J., Wang, P., 2020b. The aggregation kinetics of manganese oxides nanoparticles in Al(III) electrolyte solutions: roles of distinct Al (III) species and natural organic matters. Sci. Total Environ. 744, 140814.

Chowdhury, I., Duch, M.C., Mansukhani, N.D., Hersam, M.C., Bouchard, D., 2013. Colloidal properties and stability of graphene oxide nanomaterials in the aquatic environment. Environ. Sci. Technol. 47, 6288–6296.

Clavier, A., Carnal, F., Stoll, S., 2016. Effect of surface and salt properties on the ion distribution around spherical nanoparticles: Monte Carlo simulations. J. Phys. Chem. B 120, 7988–7997.

Ding, Y., Sheng, A., Liu, F., Li, X., Shang, J., Liu, J., 2021. Reversing the order of changes in environmental conditions alters the aggregation behavior of hematite nanoparticles. Environ. Sci. Nano 8, 3820–3832.

Dong, F., Zhou, Y., 2020. Distinct mechanisms in the heteroaggregation of silver nanoparticles with mineral and microbial colloids. Water Res. 170, 115332.

Duan, Z., Wang, P., Yu, G., Liang, M., Dong, J., Su, J., Huang, W., Li, Y., Zhang, A., Chen, C., 2021. Aggregation kinetics of UV-aged soot nanoparticles in wet environments: effects of irradiation time and background solution chemistry. Water Res. 201, 117385.

Feng, F., Lei, T., Zhao, N., 2021. Tunable depletion force in active and crowded environments. Phys. Rev. E 103, 022604.

Feng, Y., Huynh, K.A., Xie, Z., Liu, G., Gao, S., 2019. Heteroaggregation and sedimentation of graphene oxide with hematite colloids: influence of water constituents and impact on tetracycline adsorption. Sci. Total Environ. 647, 708–715.

Feng, Y., Liu, X., Huynh, K.A., McCaffery, J.M., Mao, L., Gao, S., Chen, K.L., 2017. Heteroaggregation of graphene oxide with nanometer-and micrometer-sized hematite colloids: influence on nanohybrid aggregation and microparticle sedimentation. Environ. Sci. Technol. 51, 6821–6828.

Fritz, G., Schädler, V., Willenbacher, N., Wagner, N.J., 2002. Electrosteric stabilization of colloidal dispersions. Langmuir 18, 6381–6390.

Ghosh, S., Guo, Q., Wang, Z., Zhang, D., Pradhan, N.R., Pan, B., Xing, B., 2019. Tannic acid- and cation-mediated interfacial self-assembly and epitaxial growth of fullerene (nC60) and kaolinite binary graphitic aggregates. J. Colloid Interface Sci. 556, 717–725.

Ghosh, S., Pradhan, N.R., Mashayekhi, H., Dickert, S., Thantirige, R., Tuominen, M.T., Tao, S., Xing, B., 2014. Binary short-range colloidal assembly of magnetic iron oxides nanoparticles and fullerene (nC60) in environmental media. Environ. Sci. Technol. 48, 12285–12291.

Ghosh, S., Pradhan, N.R., Mashayekhi, H., Zhang, Q., Pan, B., Xing, B., 2016. Colloidal aggregation and structural assembly of aspect ratio variant goethite (α-FeOOH) with nC60 fullerene in environmental media. Environ. Pollut. 219, 1049–1059.

Grasso, D., Subramaniam, K., Butkus, M., Strevett, K., Bergendahl, J., 2002. A review of non-DLVO interactions in environmental colloidal systems. Rev. Environ. Sci. Biotechnol. 1, 17–38.

Grillo, R., Rosa, A.H., Fraceto, L.F., 2015. Engineered nanoparticles and organic matter: a review of the state-of-the-art. Chemosphere 119, 608–619.

Gui, X., Song, B., Chen, M., Xu, X., Ren, Z., Li, X., Cao, X., 2021. Soil colloids affect the aggregation and stability of biochar colloids. Sci. Total Environ. 771, 145414.

Guo, B., Jiang, J., Serem, W., Sharma, V.K., Ma, X., 2019. Attachment of cerium oxide nanoparticles of different surface charges to kaolinite: molecular and atomic mechanisms. Environ. Res. 177, 108645.

Guo, Q., Wang, Z., Xu, Q., Mao, H., Zhang, D., Ghosh, S., Pradhan, N.R., Pan, B., Xing, B., 2020. Suspended state heteroaggregation kinetics of kaolinite and fullerene (nC60) in the presence of tannic acid: effect of π-π interactions. Sci. Total Environ. 713, 136559.

Gupta, G.S., Senapati, V.A., Dhawan, A., Shanker, R., 2017. Heteroagglomeration of zinc oxide nanoparticles with clay mineral modulates the bioavailability and toxicity of nanoparticle in Tetrahymena pyriformis. J. Colloid Interface Sci. 495, 9–18.

Han, Z., Zhang, F., Lin, D., Xing, B., 2008. Clay minerals affect the stability of surfactant-facilitated carbon nanotube suspensions. Environ. Sci. Technol. 42, 6869–6875.

He, Y.T., Wan, J., Tokunaga, T., 2008. Kinetic stability of hematite nanoparticles: the effect of particle sizes. J. Nano Res. 10, 321–332.

Heidmann, I., Christl, I., Kretzschmar, R., 2005. Aggregation kinetics of kaolinite−fulvic acid colloids as affected by the sorption of Cu and Pb. Environ. Sci. Technol. 39, 807–813.

Hermansson, M., 1999. The DLVO theory in microbial adhesion. Colloids Surf., B 14, 105–119.

Hochella, M.F., Mogk, D.W., Ranville, J., Allen, I.C., Luther, G.W., Marr, L.C., McGrail, B. P., Murayama, M., Qafoku, N.P., Rosso, K.M., 2019. Natural, incidental, and engineered nanomaterials and their impacts on the Earth system. Science 363.

Hochella, M.F., Spencer, M.G., Jones, K.L., 2015. Nanotechnology: nature's gift or scientists' brainchild? Environ. Sci. Nano 2, 114–119.

Hoek, E.M.V., Agarwal, G.K., 2006. Extended DLVO interactions between spherical particles and rough surfaces. J. Colloid Interface Sci. 298, 50–58.

Hong, Y., Honda, R.J., Myung, N.V., Walker, S.L., 2009. Transport of iron-based nanoparticles: role of magnetic properties. Environ. Sci. Technol. 43, 8834–8839.

Hotze, E.M., Phenrat, T., Lowry, G.V., 2010. Nanoparticle aggregation: challenges to understanding transport and reactivity in the environment. J. Environ. Qual. 39, 1909–1924.

Hu, J.D., Zevi, Y., Kou, X.M., Xiao, J., Wang, X.J., Jin, Y., 2010a. Effect of dissolved organic matter on the stability of magnetite nanoparticles under different pH and ionic strength conditions. Sci. Total Environ. 408, 3477–3489.

Hu, J., Zevi, Y., Kou, X., Xiao, J., Wang, X., Jin, Y., 2010b. Effect of dissolved organic matter on the stability of magnetite nanoparticles under different pH and ionic strength conditions. Sci. Total Environ. 408, 3477–3489.

Hu, Y., Yang, Q., Kou, J., Sun, C., Li, H., 2020. Aggregation mechanism of colloidal kaolinite in aqueous solutions with electrolyte and surfactants. PLoS One 15, e0238350.

Huang, B., Wei, Z.B., Yang, L.Y., Pan, K., Miao, A.J., 2019. Combined toxicity of silver nanoparticles with hematite or plastic nanoparticles toward two freshwater algae. Environ. Sci. Technol. 53, 3871–3879.

Huang, G., Guo, H., Zhao, J., Liu, Y., Xing, B., 2016. Effect of co-existing kaolinite and goethite on the aggregation of graphene oxide in the aquatic environment. Water Res. 102, 313–320.

Huynh, K.A., Chen, K.L., 2014. Disaggregation of heteroaggregates composed of multiwalled carbon nanotubes and hematite nanoparticles. Environ. Sci.: Process. Impacts 16, 1371–1378.

Huynh, K.A., McCaffery, J.M., Chen, K.L., 2012. Heteroaggregation of multiwalled carbon nanotubes and hematite nanoparticles: rates and mechanisms. Environ. Sci. Technol. 46, 5912–5920.

Huynh, K.A., McCaffery, J.M., Chen, K.L., 2014. Heteroaggregation reduces antimicrobial activity of silver nanoparticles: evidence for nanoparticle–cell proximity effects. Environ. Sci. Technol. Lett. 1, 361–366.

Islam, A.M., Chowdhry, B.Z., Snowden, M.J., 1995. Heteroaggregation in colloidal dispersions. Adv. Colloid Interface Sci. 62, 109–136.

Jing, F., Sun, Y., Liu, Y., Wan, Z., Chen, J., Tsang, D.C.W., 2021. Interactions between biochar and clay minerals in changing biochar carbon stability. Sci. Total Environ., 151124

Junaid, M., Wang, J., 2021. Interaction of micro(nano)plastics with extracellular and intracellular biomolecules in the freshwater environment. Crit. Rev. Environ. Sci. Technol. 1–25.

Kansara, K., Paruthi, A., Misra, S.K., Karakoti, A.S., Kumar, A., 2019. Montmorillonite clay and humic acid modulate the behavior of copper oxide nanoparticles in aqueous environment and induces developmental defects in zebrafish embryo. Environ. Pollut. 255, 113313.

Keller, A.A., Wang, H., Zhou, D., Lenihan, H.S., Cherr, G., Cardinale, B.J., Miller, R., Ji, Z., 2010. Stability and aggregation of metal oxide nanoparticles in natural aqueous matrices. Environ. Sci. Technol. 44, 1962–1967.

Labille, J., Harns, C., Bottero, J.-Y., Brant, J., 2015. Heteroaggregation of titanium dioxide nanoparticles with natural clay colloids. Environ. Sci. Technol. 49, 6608–6616.

Landman, J., Schelling, M.P.M., Tuinier, R., Vis, M., 2021. Repulsive and attractive depletion forces mediated by nonadsorbing polyelectrolytes in the Donnan limit. J. Chem. Phys. 154, 164904.
Li, S., Sun, W., 2011. A comparative study on aggregation/sedimentation of TiO2 nanoparticles in mono- and binary systems of fulvic acids and Fe(III). J. Hazard Mater. 197, 70–79.
Li, X., He, E., Zhang, M., Peijnenburg, W.J.G.M., Liu, Y., Song, L., Cao, X., Zhao, L., Qiu, H., 2020a. Interactions of CeO2 nanoparticles with natural colloids and electrolytes impact their aggregation kinetics and colloidal stability. J. Hazard Mater. 386, 121973.
Li, Y., Wang, X., Fu, W., Xia, X., Liu, C., Min, J., Zhang, W., Crittenden, J.C., 2019. Interactions between nano/micro plastics and suspended sediment in water: implications on aggregation and settling. Water Res. 161, 486–495.
Li, Z., Shakiba, S., Deng, N., Chen, J., Louie, S.M., Hu, Y., 2020b. Natural organic matter (NOM) imparts molecular-weight-dependent steric stabilization or electrostatic destabilization to ferrihydrite nanoparticles. Environ. Sci. Technol. 54, 6761–6770.
Lian, F., Yu, W., Wang, Z., Xing, B., 2019. New insights into black carbon nanoparticle-induced dispersibility of goethite colloids and configuration-dependent sorption for Phenanthrene. Environ. Sci. Technol. 53, 661–670.
Liao, P., Li, W., Wang, D., Jiang, Y., Pan, C., Fortner, J.D., Yuan, S., 2017. Effect of reduced humic acid on the transport of ferrihydrite nanoparticles under anoxic conditions. Water Res. 109, 347–357.
Lin, D., Cai, P., Peacock, C.L., Wu, Y., Gao, C., Peng, W., Huang, Q., Liang, W., 2018. Towards a better understanding of the aggregation mechanisms of iron (hydr)oxide nanoparticles interacting with extracellular polymeric substances: role of pH and electrolyte solution. Sci. Total Environ. 645, 372–379.
Liu, G., Zheng, H., Jiang, Z., Wang, Z., 2018a. Effects of biochar input on the properties of soil nanoparticles and dispersion/sedimentation of natural mineral nanoparticles in aqueous phase. Sci. Total Environ. 634, 595–605.
Liu, G., Zheng, H., Jiang, Z., Zhao, J., Wang, Z., Pan, B., Xing, B., 2018b. Formation and physicochemical characteristics of nano biochar: insight into chemical and colloidal stability. Environ. Sci. Technol. 52, 10369–10379.
Liu, J., Dai, C., Hu, Y., 2018c. Aqueous aggregation behavior of citric acid coated magnetite nanoparticles: effects of pH, cations, anions, and humic acid. Environ. Res. 161, 49–60.
Liu, J., Hwang, Y.S., Lenhart, J.J., 2015. Heteroaggregation of bare silver nanoparticles with clay minerals. Environ. Sci. Nano 2, 528–540.
Liu, J., Louie, S.M., Pham, C., Dai, C., Liang, D., Hu, Y., 2019a. Aggregation of ferrihydrite nanoparticles: effects of pH, electrolytes,and organics. Environ. Res. 172, 552–560.
Liu, X., Li, J., Huang, Y., Wang, X., Zhang, X., Wang, X., 2017. Adsorption, aggregation, and deposition behaviors of carbon dots on minerals. Environ. Sci. Technol. 51, 6156–6164.
Liu, Y., Hu, Y., Yang, C., Chen, C., Huang, W., Dang, Z., 2019b. Aggregation kinetics of UV irradiated nanoplastics in aquatic environments. Water Res. 163, 114870.
Liu, Y., Huang, Z., Zhou, J., Tang, J., Yang, C., Chen, C., Huang, W., Dang, Z., 2020. Influence of environmental and biological macromolecules on aggregation kinetics of nanoplastics in aquatic systems. Water Res. 186, 116316.
Lowry, G.V., Gregory, K.B., Apte, S.C., Lead, J.R., 2012. Transformations of nanomaterials in the environment. Environ. Sci. Technol. 46, 6893–6899.
Lv, B., Wang, C., Hou, J., Wang, P., Miao, L., Xing, B., 2020. Development of a comprehensive understanding of aggregation-settling movement of CeO2 nanoparticles in natural waters. Environ. Pollut. 257, 113584.
Ma, J., Jing, Y., Gao, L., Chen, J., Wang, Z., Weng, L., Li, H., Chen, Y., Li, Y., 2020. Hetero-aggregation of goethite and ferrihydrite nanoparticles controlled by goethite nanoparticles with elongated morphology. Sci. Total Environ. 748, 141536.
Marenduzzo, D., Finan, K., Cook, P.R., 2006. The depletion attraction: an underappreciated force driving cellular organization. J. Cell Biol. 175, 681–686.
Mukherjee, R., Kumar, R., Sinha, A., Lama, Y., Saha, A.K., 2016. A review on synthesis, characterization, and applications of nano zero valent iron (nZVI) for environmental remediation. Crit. Rev. Environ. Sci. Technol. 46, 443–466.
Oriekhova, O., Stoll, S., 2019. Heteroaggregation of CeO2 nanoparticles in presence of alginate and iron(III) oxide. Sci. Total Environ. 648, 1171–1178.
Palomino, D., Stoll, S., 2013a. Fulvic acids concentration and pH influence on the stability of hematite nanoparticles in aquatic systems. J. Nano Res. 15, 1428.
Palomino, D., Stoll, S., 2013b. Fulvic acids concentration and pH influence on the stability of hematite nanoparticles in aquatic systems. J. Nano Res. 15.
Parsai, T., Kumar, A., 2020. Stability and characterization of mixture of three particle system containing ZnO-CuO nanoparticles and clay. Sci. Total Environ. 740, 140095.
Peijnenburg, W.J.G.M., Baalousha, M., Chen, J., Chaudry, Q., Von der kammer, F., Kuhlbusch, T.A.J., Lead, J., Nickel, C., Quik, J.T.K., Renker, M., Wang, Z., Koelmans, A.A., 2015. A review of the properties and processes determining the fate of engineered nanomaterials in the aquatic environment. Crit. Rev. Environ. Sci. Technol. 45, 2084–2134.
Petosa, A.R., Jaisi, D.P., Quevedo, I.R., Elimelech, M., Tufenkji, N., 2010. Aggregation and deposition of engineered nanomaterials in aquatic environments: role of physicochemical interactions. Environ. Sci. Technol. 44, 6532–6549.
Phenrat, T., Saleh, N., Sirk, K., Tilton, R.D., Lowry, G.V., 2007. Aggregation and sedimentation of aqueous nanoscale zerovalent iron dispersions. Environ. Sci. Technol. 41, 284–290.
Philippe, A., Schaumann, G.E., 2014. Interactions of dissolved organic matter with natural and engineered inorganic colloids: a review. Environ. Sci. Technol. 48, 8946–8962.
PlasticsEurope, 2021. Plastics - the Facts 2021. An Analysis of European Plastics Production, Demand and Waste Data. http://www.plasticseurope.
Praetorius, A., Labille, J., Scheringer, M., Thill, A., Hungerbühler, K., Bottero, J.-Y., 2014. Heteroaggregation of titanium dioxide nanoparticles with model natural colloids under environmentally relevant conditions. Environ. Sci. Technol. 48, 10690–10698.
Quik, J.T.K., Velzeboer, I., Wouterse, M., Koelmans, A.A., van de Meent, D., 2014. Heteroaggregation and sedimentation rates for nanomaterials in natural waters. Water Res. 48, 269–279.
Romero-Cano, M.S., Martín-Rodríguez, A., de las Nieves, F.J., 2001. Electrosteric stabilization of polymer colloids with different functionality. Langmuir 17, 3505–3511.
Sabaraya, I.V., Shin, H., Li, X., Hoq, R., Incorvia, J.A.C., Kirisits, M.J., Saleh, N.B., 2021. Role of electrostatics in the heterogeneous interaction of two-dimensional engineered MoS2 nanosheets and natural clay colloids: influence of pH and natural organic matter. Environ. Sci. Technol. 55, 919–929.
Shao, Z., Luo, S., Liang, M., Ning, Z., Sun, W., Zhu, Y., Mo, J., Li, Y., Huang, W., Chen, C., 2021. Colloidal stability of nanosized activated carbon in aquatic systems: effects of pH, electrolytes, and macromolecules. Water Res. 203, 117561.
Sharma, V.K., Filip, J., Zboril, R., Varma, R.S., 2015. Natural inorganic nanoparticles – formation, fate, and toxicity in the environment. Chem. Soc. Rev. 44, 8410–8423.
Shen, C., Wu, L., Zhang, S., Ye, H., Li, B., Huang, Y., 2014. Heteroaggregation of microparticles with nanoparticles changes the chemical reversibility of the microparticles' attachment to planar surfaces. J. Colloid Interface Sci. 421, 103–113.
Sheng, A., Liu, F., Shi, L., Liu, J., 2016a. Aggregation kinetics of hematite particles in the presence of outer membrane cytochrome OmcA of Shewanella oneidenesis MR-1. Environ. Sci. Technol. 50, 11016–11024.
Sheng, A., Liu, F., Xie, N., Liu, J., 2016b. Impact of proteins on aggregation kinetics and adsorption ability of hematite nanoparticles in aqueous dispersions. Environ. Sci. Technol. 50, 2228–2235.
Shrestha, S., Wang, B., Dutta, P., 2020. Nanoparticle processing: understanding and controlling aggregation. Adv. Colloid Interface Sci. 279, 102162.
Singh, N., Tiwari, E., Khandelwal, N., Darbha, G.K., 2019. Understanding the stability of nanoplastics in aqueous environments: effect of ionic strength, temperature, dissolved organic matter, clay, and heavy metals. Environ. Sci. Nano 6, 2968–2976.
Smith, B.M., Pike, D.J., Kelly, M.O., Nason, J.A., 2015. Quantification of heteroaggregation between citrate-stabilized gold nanoparticles and hematite colloids. Environ. Sci. Technol. 49, 12789–12797.
Sotirelis, N.P., Chrysikopoulos, C.V., 2017. Heteroaggregation of graphene oxide nanoparticles and kaolinite colloids. Sci. Total Environ. 579, 736–744.
Sun, B., Zhang, Y., Chen, W., Wang, K., Zhu, L., 2018. Concentration dependent effects of bovine serum albumin on graphene oxide colloidal stability in aquatic environment. Environ. Sci. Technol. 52, 7212–7219.
Sun, B., Zhang, Y., Li, R., Wang, K., Xiao, B., Yang, Y., Wang, J., Zhu, L., 2021a. New insights into the colloidal stability of graphene oxide in aquatic environment: interplays of photoaging and proteins. Water Res. 200, 117213.
Sun, B., Zhang, Y., Liu, Q., Yan, C., Xiao, B., Yang, J., Liu, M., Zhu, L., 2020a. Lateral size dependent colloidal stability of graphene oxide in water: impacts of protein properties and water chemistry. Environ. Sci. Nano 7, 634–644.
Sun, B., Zhang, Y., Liu, X., Wang, K., Yang, Y., Zhu, L., 2022. Impacts of photoaging on the interactions between graphene oxide and proteins: mechanisms and biological effect. Water Res. 216, 118371.
Sun, H., Jiao, R., An, G., Xu, H., Wang, D., 2021b. Influence of particle size on the aggregation behavior of nanoparticles: role of structural hydration layer. J. Environ. Sci. (China) 103, 33–42.
Sun, H., Jiao, R., An, G., Xu, H., Wang, D., 2021c. Influence of particle size on the aggregation behavior of nanoparticles: role of structural hydration layer. J. Environ. Sci. 103, 33–42.
Sun, W.L., Zhou, K., 2014. Adsorption of 17 beta-estradiol by multi-walled carbon nanotubes in natural waters with or without aquatic colloids. Chem. Eng. J. 258, 185–193.
Sun, Y., Pan, D., Wei, X., Xian, D., Wang, P., Hou, J., Xu, Z., Liu, C., Wu, W., 2020b. Insight into the stability and correlated transport of kaolinite colloid: effect of pH, electrolytes and humic substances. Environ. Pollut. 266, 115189.
Tang, S.C.N., Lo, I.M.C., 2013. Magnetic nanoparticles: essential factors for sustainable environmental applications. Water Res. 47, 2613–2632.
Tang, Z., Cheng, T., Fisher-Power, L.M., 2018. Influence of aggregation on nanoscale titanium dioxide (nTiO2) deposition to quartz sand. Chemosphere 209, 517–524.
Therezien, M., Thill, A., Wiesner, M.R., 2014. Importance of heterogeneous aggregation for NP fate in natural and engineered systems. Sci. Total Environ. 485–486, 309–318.
Tombácz, E., Szekeres, M., 2006. Surface charge heterogeneity of kaolinite in aqueous suspension in comparison with montmorillonite. Appl. Clay Sci. 34, 105–124.
Uddin, M.K., 2017. A review on the adsorption of heavy metals by clay minerals, with special focus on the past decade. Chem. Eng. J. 308, 438–462.
Upendar, S., Mani, E., Basavaraj, M.G., 2018. Aggregation and stabilization of colloidal spheroids by oppositely charged spherical nanoparticles. Langmuir 34, 6511–6521.
van Oss, C.J., 1993. Acid—base interfacial interactions in aqueous media. Colloids Surfaces A Physicochem. Eng. Asp. 78, 1–49.
van Riemsdijk, W.H., Koopal, L.K., Kinniburgh, D.G., Benedetti, M.F., Weng, L., 2006. Modeling the interactions between humics, ions, and mineral surfaces. Environ. Sci. Technol. 40, 7473–7480.
Velzeboer, I., Quik, J.T., van de Meent, D., Koelmans, A.A., 2014. Rapid settling of nanoparticles due to heteroaggregation with suspended sediment. Environ. Toxicol. Chem. 33, 1766–1773.
Vikesland, P.J., Rebodos, R.L., Bottero, J.Y., Rose, J., Masion, A., 2016. Aggregation and sedimentation of magnetite nanoparticle clusters. Environ. Sci. Nano 3, 567–577.

Vindedahl, A.M., Stemig, M.S., Arnold, W.A., Penn, R.L., 2016. Character of humic substances as a predictor for goethite nanoparticle reactivity and aggregation. Environ. Sci. Technol. 50, 1200–1208.
Wang, H., Adeleye, A.S., Huang, Y., Li, F., Keller, A.A., 2015a. Heteroaggregation of nanoparticles with biocolloids and geocolloids. Adv. Colloid Interface Sci. 226, 24–36.
Wang, H., Dong, Y.-n., Zhu, M., Li, X., Keller, A.A., Wang, T., Li, F., 2015b. Heteroaggregation of engineered nanoparticles and kaolin clays in aqueous environments. Water Res. 80, 130–138.
Wang, H., Zhao, X., Han, X., Tang, Z., Liu, S., Guo, W., Deng, C., Guo, Q., Wang, H., Wu, F., Meng, X., Giesy, J.P., 2017. Effects of monovalent and divalent metal cations on the aggregation and suspension of Fe3O4 magnetic nanoparticles in aqueous solution. Sci. Total Environ. 586, 817–826.
Wang, H., Zhao, X., Han, X., Tang, Z., Song, F., Zhang, S., Zhu, Y., Guo, W., He, Z., Guo, Q., Wu, F., Meng, X., Giesy, J.P., 2018a. Colloidal stability of Fe3O4 magnetic nanoparticles differentially impacted by dissolved organic matter and cations in synthetic and naturally-occurred environmental waters. Environ. Pollut. 241, 912–921.
Wang, J., Guo, X., Xue, J., 2021a. Biofilm-developed microplastics as vectors of pollutants in aquatic environments. Environ. Sci. Technol. 55, 12780–12790.
Wang, J., Zhao, X., Wu, F., Tang, Z., Zhao, T., Niu, L., Fang, M., Wang, H., Wang, F., 2021b. Impact of montmorillonite clay on the homo- and heteroaggregation of titanium dioxide nanoparticles (nTiO2) in synthetic and natural waters. Sci. Total Environ. 784, 147019.
Wang, X., Zhang, D., Qian, H., Liang, Y., Pan, X., Gadd, G.M., 2018b. Interactions between biogenic selenium nanoparticles and goethite colloids and consequence for remediation of elemental mercury contaminated groundwater. Sci. Total Environ. 613–614, 672–678.
Wang, Y., Yang, K., Chefetz, B., Xing, B., Lin, D., 2019a. The pH and concentration dependent interfacial interaction and heteroaggregation between nanoparticulate zero-valent iron and clay mineral particles. Environ. Sci. Nano 6, 2129–2140.
Wang, Y., Zhang, W., Shang, J., Shen, C., Joseph, S.D., 2019b. Chemical aging changed aggregation kinetics and transport of biochar colloids. Environ. Sci. Technol. 53, 8136–8146.
Weng, L., Van Riemsdijk, W.H., Hiemstra, T., 2007. Adsorption of humic acids onto goethite: effects of molar mass, pH and ionic strength. J. Colloid Interface Sci. 314, 107–118.
Wu, S., Liu, C., Li, X., Xiao, B., Hu, Q., 2022. Freeze-thaw controlled aggregation mechanism of humic acid-coated goethite: implications for organic carbon preservation. Geoderma 406, 115514.
Xu, C.Y., Deng, K.Y., Li, J.Y., Xu, R.K., 2015a. Impact of environmental conditions on aggregation kinetics of hematite and goethite nanoparticles. J. Nano Res. 17, 394.
Xu, C.Y., Zhou, T.T., Wang, C.L., Liu, H.Y., Zhang, C.T., Hu, F.N., Zhao, S.W., Geng, Z.C., 2020. Aggregation of polydisperse soil colloidal particles: dependence of Hamaker constant on particle size. Geoderma 359, 113999.
Xu, C., Deng, K., Li, J., Xu, R., 2015b. Impact of environmental conditions on aggregation kinetics of hematite and goethite nanoparticles. J. Nano Res. 17, 394.
Yan, C., Cheng, T., Shang, J., 2019. Effect of bovine serum albumin on stability and transport of kaolinite colloid. Water Res. 155, 204–213.
Yang, F., Xu, Z., Yu, L., Gao, B., Xu, X., Zhao, L., Cao, X., 2018. Kaolinite enhances the stability of the dissolvable and undissolvable fractions of biochar via different mechanisms. Environ. Sci. Technol. 52, 8321–8329.
Yang, Z., Yan, H., Yang, H., Li, H., Li, A., Cheng, R., 2013. Flocculation performance and mechanism of graphene oxide for removal of various contaminants from water. Water Res. 47, 3037–3046.
Yi, P., Chen, K.L., 2013. Influence of solution chemistry on the release of multiwalled carbon nanotubes from silica surfaces. Environ. Sci. Technol. 47, 12211–12218.
Zhang, H., Taujale, S., Huang, J., Lee, G.J., 2015. Effects of NOM on oxidative reactivity of manganese dioxide in binary oxide mixtures with goethite or hematite. Langmuir 31, 2790–2799.
Zhang, L., Petersen, E.J., Zhang, W., Chen, Y., Cabrera, M., Huang, Q., 2012. Interactions of 14C-labeled multi-walled carbon nanotubes with soil minerals in water. Environ. Pollut. 166, 75–81.
Zhang, W., Rattanaudompol, U.s., Li, H., Bouchard, D., 2013. Effects of humic and fulvic acids on aggregation of aqu/nC60 nanoparticles. Water Res. 47, 1793–1802.
Zhang, Y., Luo, Y., Guo, X., Xia, T., Wang, T., Jia, H., Zhu, L., 2020. Charge mediated interaction of polystyrene nanoplastic (PSNP) with minerals in aqueous phase. Water Res. 178, 115861.
Zhao, J., Li, Y., Wang, X., Xia, X., Shang, E., Ali, J., 2021a. Ionic-strength-dependent effect of suspended sediment on the aggregation, dissolution and settling of silver nanoparticles. Environ. Pollut. 279, 116926.
Zhao, J., Liu, F., Wang, Z., Cao, X., Xing, B., 2015. Heteroaggregation of graphene oxide with minerals in aqueous phase. Environ. Sci. Technol. 49, 2849–2857.
Zhao, J., Tang, J., Dang, T., 2021b. Influence of extracellular polymeric substances on the heteroaggregation between CeO2 nanoparticles and soil mineral particles. Sci. Total Environ., 150358
Zhou, D., Abdel-Fattah, A.I., Keller, A.A., 2012. Clay particles destabilize engineered nanoparticles in aqueous environments. Environ. Sci. Technol. 46, 7520–7526.
Zhu, L., Li, Z., Tian, R., Li, H., 2019. Specific ion effects of divalent cations on the aggregation of positively charged goethite nanoparticles in aqueous suspension. Colloids Surfaces A Physicochem. Eng. Asp. 565, 78–85.
Zhu, M., Wang, H., Keller, A.A., Wang, T., Li, F., 2014. The effect of humic acid on the aggregation of titanium dioxide nanoparticles under different pH and ionic strengths. Sci. Total Environ. 487, 375–380.